eLife

Reviewed Preprint
v1 • July 31, 2026
Not revised

For correspondence:
gbucher1@uni-goettingen.de

Competing interests: The co-author Bastian Klußmann-Fricke is employee of the company Abberior, the STED device of which we have used to gather some data. The company had no influence on the scientific question, the approach and the interpretation of the data.

Funding: See page 23

Reviewing editor: Gáspár Jékely, Heidelberg University, Germany

foxQ2 marks fast-acting brain interneurons including a subset of dopaminergic neurons innervating *mushroom bodies* and *central complex* in the beetle *Tribolium castaneum*

Ying Pang[1], Bastian Klußmann-Fricke[3], Doga Cedden[1], Jiajun Zhang[2], Johannes B Schinko[1,4], Michalis Averof[4], Thomas Riemensperger[2], Gregor Bucher[1]

[1]University of Göttingen, Department of Evolutionary Developmental Genetics, GZMB, Göttingen, Germany • [2]Institute of Zoology, University of Cologne, Köln, Germany • [3]Abberior Instruments GmbH, Göttingen, Germany • [4]Institut de Génomique Fonctionnelle de Lyon (IGFL), École Normale Supérieure de Lyon, Lyon, France

eLife Assessment

This **valuable** descriptive study describes the expression of a developmentally relevant transcription factor in the adult Tribolium brain. The evidence supporting the claims is **convincing** and based on a very detailed and rigorous analysis of light microscopy data, which, however, lacks single-cell resolution. This neuroanatomical study is of interest to the field of insect neural development and neuroscience.

https://doi.org/10.7554/eLife.111703.1.sa3

Abstract

The brain is one of the most complex animal organs but the development of the many different neuron types remains enigmatic. A set of brain-specific transcription factors is known to be involved in brain patterning but their specific contributions remain to be elucidated in most cases, including *foxQ2II*. This transcription factor is known to be conserved in anterior neuroectodermal patterning of most animals while it has been lost from vertebrates. However, the contribution of *foxQ2II*-positive neurons to the adult brain has remained enigmatic. Here, we use an enhancer trap, immunostainings and our newly established beetle *brainbow* system to categorize *Tc-foxQ2II*-positive neurons into nine clusters with different projection patterns. All clusters contain neurons with the fast activating neurotransmitters acetylcholine and glutamate while no *Tc-foxQ2II* positive neuron is GABA-ergic or serotonin-positive. Interestingly, we found that many dopaminergic neurons were *Tc-foxQ2II* positive and we homologize them with dopaminergic neurons of the PPL2c, PPM1 and PPL1 cluster described in the *Drosophila* brain. Our results show that *Tc-foxQ2II* marks subsets of fast-acting interneurons contributing to the higher order brain centers *mushroom bodies* and *central complex*. Taken together, our work expands the known functional range of *foxQ2* genes from sensory and neurosecretory cell specification to interneurons involved in the function of higher order brain centers.

Introduction

The brain is built by a plethora of different neural cell types, which are interconnected in a very complex yet strictly ordered way. How this complexity develops and how the neural cell types are specified remains one of the major enigmas of developmental biology. Insects have served as an important model organism to understand basic principles of brain development because they have comparably simple brains and are experimentally more accessible than vertebrates.

Especially the fruit fly *Drosophila melanogaster* has served as excellent model organism to pioneer molecular and genetic insights into nervous system development (Bellen et al., 2010). In contrast to the brain, extensive research has revealed the principles of neural pattern formation and genetic signals of cell specification in the ventral nerve cord (Skeath and Thor, 2003; Urbach and Technau, 2004). In brief, the segmental neuroectoderm is subdivided by an orthogonal grid formed by the expression of columnar and segment polarity genes while Hox gene expression conveys regional identity. When the neural stem cells (neuroblasts, NBs) delaminate from the neuroectoderm, they inherit this spatial pattern of transcription factors from the neuroectoderm (e.g. different combinations of columnar, segment polarity and other genes). This "transcription factor cocktail" confers different identities to the delaminating NBs, which subsequently develop cell-autonomously into different neural lineages. On top of this spatial patterning, further neural cell diversification occurs e.g. by temporal patterning and lateral inhibition (Miyares and Lee, 2019; Skeath and Thor, 2003; Truman et al., 2010). In holometabolous insects, the embryonic phase of brain development leads to a simplified but functional larval brain. Postembryonic development adds to the scaffold provided by the larval brain and eventually leads to the formation of the adult brain (Hartenstein et al., 2008; Truman and Riddiford, 2023).

The insect brain is composed of three neuromeres, which stem from different neuroectodermal regions. The tritocerebrum and deutocerebrum derive from the intercalary and antennal segments, respectively. Due to their segmental origin, the basic principles of patterning these neuromeres are likely to be similar to the ventral nerve cord and indeed the expression of patterning genes in their NBs is similar (Urbach and Technau, 2003b; Urbach and Technau, 2004). The protocerebrum differs from the segmented ventral nerve cord in several respects. It contains crucial neuropils not found more posteriorly such as *mushroom bodies*, *central complex* and *optic lobes*. Further, it is built by a much larger pool of NBs and in addition to type I neuroblasts, which build the VNC, the brain additionally contains some type II NBs. These NBs produce more offspring by producing intermediate neural progenitors, which themselves divide in a stem cell like fashion and contribute to the central complex (Bello et al., 2008; Boone and Doe, 2008; Boyan et al., 2010; Walsh and Doe, 2017). We and others have argued that the protocerebrum derives from the anterior non-segmental part of the neuroectoderm and evolutionary predated the segmentally organized ganglia. This lends an evolutionary explanation for pronounced differences with the VNC (Posnien et al., 2023; Scholtz and Edgecombe, 2006).

Molecular divergence reflects these differences and in contrast to the VNC, the genes and interactions involved in brain development are much less comprehensively studied (Kunz et al., 2012; Urbach and Technau, 2003b; Urbach et al., 2003). It is clear, however, that a different set of genes must be involved because the Hox genes and most columnar and segment polarity genes are not expressed in the anterior-most region of the embryo. Instead, a different set of highly conserved transcription factors is involved in anterior head and brain patterning in all animals (Gehring and Ikeo, 1999; Hirth et al., 2003; Leclère et al., 2016; Posnien et al., 2011; Posnien et al., 2023; Simeone et al., 1992; Sinigaglia et al., 2022; Tomer et al., 2010). The regulatory input by this set of uniquely anterior genes likely contributes to the development and specification of insect brain-specific structures such as central complex, mushroom body and optic lobe neuropils (Posnien et al., 2023). However, the function of most of these genes in insect brain development remains unknown.

Some *foxQ2* gene family transcription factors are involved in early anterior and neural patterning. Three members of the *foxQ2* family were ancestrally present in the sister group to bilaterian animals, the cnidarians. A complex pattern of losses led to a situation where the *foxQ2II* family is the only one retained in many protostomes (e.g. arthropods, nematodes) while it had been lost in tunicates and vertebrates including frogs, mice and fish (Gattoni et al., 2025b). Here, we focus on *foxQ2II*, which has been studied in many animals for its early anterior function and is the only paralog present in arthropods. In previous works in arthopods, this gene had been referred to as *foxQ2 (Tc-foxQ2* in *Tribolium)* and it corresponds to *Nematostella foxQ2a. foxQ2II* genes show an almost exclusive anterior expression in embryos of protostomes such as the fruit fly (Lee and Frasch, 2004), the red flour beetle (He et al., 2019; Kitzmann et al., 2017), spiders (Schacht et

al., 2020) and annelids (He et al., 2019; Kitzmann et al., 2017; Marlow et al., 2014). Similar polar expression is found in deuterostomes such as the sea urchin and basal chordates (Gattoni et al., 2025b; Yaguchi et al., 2008). The gene is expressed at the aboral pole in a sister clade to all bilaterian animals, the Cnidarians, indicating an ancestral function (Sinigaglia et al., 2013). Other *foxQ2* family members were found to be expressed in anterior neural calls in basal chordates and were shown to be required for retinal patterning in fish (Gattoni et al., 2025a; Gattoni et al., 2025b; Ogawa et al., 2021). Involvement in sensory cell development has been suggested for the *foxQ2d* paralog of a Cnidarian (Busengdal and Rentzsch, 2017).

While some members of the *foxQ2* family have been related to neurosecretory and sensory cell development, information on the neural types marked by *foxQ2II* has remained scarce and absent from arthropods. This includes the fly ortholog *fd102C* for which functional data has been lacking (Lee and Frasch, 2004). Actually, *Drosophila* has a rather derived mode of head development. During embryogenesis, the head and brain neuroectoderm are involuted outside-into the thorax leading to a highly diverged and reduced situation, which has been technically difficult to analyze. *Drosophila* is also derived within insects with respect to its comparably small number of brain neuroblasts (Urbach and Technau, 2003a), and its simplified larval brain, which for instance lacks a *central complex* neuropil (Koniszewski et al., 2016; Pfeiffer and Homberg, 2014). In order to study the genetic control of brain development in a more insect-typical situation, the red flour beetle *Tribolium castaneum* has been established as complementary model system (Posnien et al., 2010). The extensive toolkit available in this species includes transgenesis, genome editing, a strong RNAi response and genome-wide RNAi resources, which together allow for in depth functional studies (Klingler and Bucher, 2022). For instance, new insights have been gained into the heterochrony of the *central complex* development and a diverging number of type II neuroblasts was found compared to fly knowledge (Farnworth et al., 2020; Rethemeier et al., 2025).

In *Tribolium*, the role of *foxQ2II* has been well characterized with respect to embryonic brain development. In the embryo, *Tc-foxQ2II* is co-expressed with *six3/optix* playing a key role at the top of the anterior gene regulatory network (aGRN) (Kitzmann et al., 2017) and it interacts with other brain-specific transcription factors, such as *Tc-six3/optix*, *Tc-six4*, *Tc-chx/vsx*, *Tc-nkx2.1/scro*, *Tc-ey*, *Tc-rx* and *Tc-fez1* (Kitzmann et al., 2017). Further, *Tc-foxQ2II* is expressed in several embryonic neuroblasts, which have at least four different molecular identities based on co-expression with other genes. Probably, both type I and type II NBs are marked (He et al., 2019). RNAi knock-down prohibits the split of the primary brain commissure into several fascicles, from which parts of the *central complex* develop. This leads to severe disturbance of the *central complex* and secondarily to the aberrant arrangement of the mushroom body (He et al., 2019; Kitzmann et al., 2017). To identify the neural cells marked by *Tc-foxQ2*, an enhancer trap line was generated by genome editing. This revealed that in the larval brain, *Tc-foxQ2II* marks at least three clusters of neurons but no glia. Some neurons project into the larval *central body* among other structures (He et al., 2019).

In contrast to embryonic development, the role of *foxQ2II* during postembryonic arthropod development remains unknown. Here, we characterize the *Tc-foxQ2II* marked neurons in the adult brain. We find and characterize nine neuron clusters and we established the brainbow system in *Tribolium* to confirm projections of cell clusters by sparse marking. We found that many *Tc-foxQ2II* marked neurons project into *mushroom bodies* or *central complex*. Further, all *Tc-foxQ2II* positive neurons are positive for the fast-acting neurotransmitters acetylcholine and glutamate while we found no coexpression with GABA or serotonin. A subset is dopamine and octopamine positive including a large part (~71.2%) of the adult dopaminergic neurons, which probably correspond to fly neurons from the PPL2c, PPM1 and PPL1 clusters. Taken together, we show an important role of *foxQ2II* in the specification of interneurons while in other animal clades, sensory and neuroendocrine cell types were linked to *foxQ2*. Further, *Tc-foxQ2II* positive neurons contribute to the higher order brain centers including both, columnar and tangential neurons of the *central complex*.

Results

Tc-foxQ2II positive cells of the adult brain are organized into nine clusters

Tc-foxQ2II positive neurons contribute to the *central complex* both in the larval and the adult brain (He et al., 2019). While the larval projection pattern had been well described in *Tribolium*, detailed information on the adult brain was lacking in any insect. To close this knowledge gap, we used our established transgenic *foxQ2* imaging line (*foxQ2-5'-line*), which marks *Tc-foxQ2II* positive cells with EGFP and Cre (He et al., 2019). To check for the degree of overlap of EGFP and Tc-foxQ2II expression in adult brains, we performed double immunohistochemistry with anti-FoxQ2 and anti-GFP antibodies (He et al., 2019). We detected that 85.1% of cells expressing Tc-foxQ2II also expressed EGFP, while 79.0% of EGFP-expressing cells overlapped with Tc-foxQ2II (n= 3; Supplementary Fig. 1 A-A" and B). We concluded that the expression patterns match sufficiently to use EGFP expression of the *foxQ2-5'-line* as proxy for studying match *Tc-foxQ2II* positive cells.

We found nine *Tc-foxQ2II* positive cell clusters in the adult brain based on cell body location and their main projections (Fig. 1 A-D; Fig. 2 A,B). One additional cluster (anterior cluster, AC; white star / yellow color in Fig. 1 A', B', and Fig. 2) was not marked by the Tc-foxQ2II antibody (supplementary Fig. 2) and was therefore not considered further in this study. Three primary clusters had been assigned by He for the embryonic and larval brain (He et al., 2019): The median cluster (MC), the lateral cluster (LC) and the posterior cluster (PC). We named the nine clusters in the adult brain in accordance with this nomenclature. One brain was used for analysis and 3D reconstructions (Fig. 1, and subsequent figures) while the statements were confirmed in five additional brains (stacks for all brains shown in this work are available on FigShare *https://figshare.com/s/379a7896e38863e07aa7*).

Ipsilateral projection neurons (MC1 and MC2) located near the central complex

The neuropils reconstructed based on synapsin staining and their abbreviations are shown in Fig. 3A. The cell bodies of MC1 (magenta in Fig. 3B,B') are located above the protocerebral bridge (PB) and project two long tracts through the PB (we found no projections into the PB) towards the posterior slope (VMCpo/PS). According to the standard neuropil compartmentalization (Farnworth et al., 2022), MC1 projections traverse the inferior protocerebrum, posterior domain (IPp) and the posterior slope (VMCpo/PS), with partial projections ultimately reaching the boundary between the VMCpo/PS and the lateral accessory lobe (LAL) and arborizing within the LAL. Compared to MC1, the cell bodies of MC2 (Fig. 3 C-C') are positioned closer to the midline, residing in the central depression of the PB. Their projections do not cross the midline but extend a tract towards the VMCpo/PS and LAL.

The location of the cell bodies of MC1 neurons and their projection ventrally along the midline between the PB and the CB is similar to dopaminergic PPM1 cluster neuron from *Drosophila melanogaster* (Supplementary Fig. 3 A-A') (Hartenstein et al., 2017; Mao and Davis, 2009), typed as PPM1205 in the *Drosophila* electron microscopy dataset (Schlegel et al., 2024). MC2 neurons may equally correspond to the dopaminergic neurons of the same PPM1 cluster in adult *Drosophila* and may be assigned to the neuron PPM1204 in the *Drosophila* electron microscopy dataset (Schlegel et al., 2024).

The lateral cluster 1 comprises tangential neurons innervating the mushroom body and the central complex

The projections and location of cell bodies allowed classifying lateral clusters (LC) into four subclusters: LC1-4. The cell bodies of LC1 (Fig. 3 D-D') were located adjacent to the calyx (CA; MBs are white in Fig. 3), with their projections passing through the CA and the superior medial protocerebrum (SMP; yellow). Two different projections seem to emanate from LC1. The

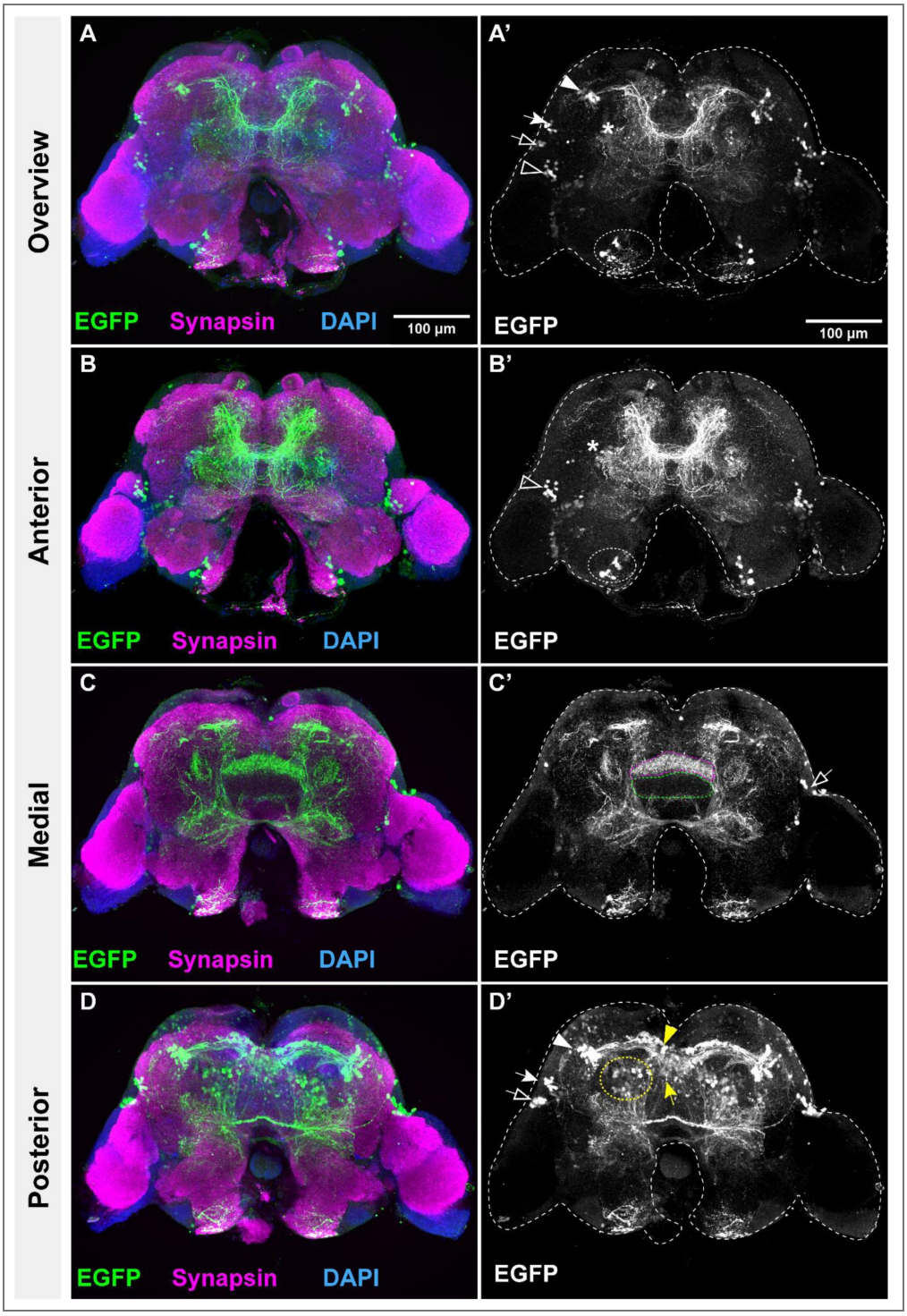

Figure 1. Overview on the *Tc-foxQ2II* positive cells.

Neuronal projection patterns were identified using immunohistochemistry against EGFP in the adult brain of *foxQ2-5'-line.* (A-D) Different parts of the adult brain stained for EGFP (green), Synapsin (magenta), and DAPI (blue). (A'-D') The EGFP channel is shown with the brain outline indicated by dashed lines. (A-A') Overview of a projection of the entire brain; (B-B') anterior subsection; (C-C') medial subsection; (D-D') posterior subsection. White arrowhead: Lateral Cluster 1; white arrow: Lateral Cluster 2; open arrowhead: Lateral Cluster 3; open arrow: Lateral Cluster 4; yellow arrowhead: Median Cluster 1; yellow arrow: Median Cluster 2; yellow dashed circle: Posterior Cluster; white dashed circle: Tritocerebrum Cluster; white star: Anterior Cluster. Scale bar: 100 µm.

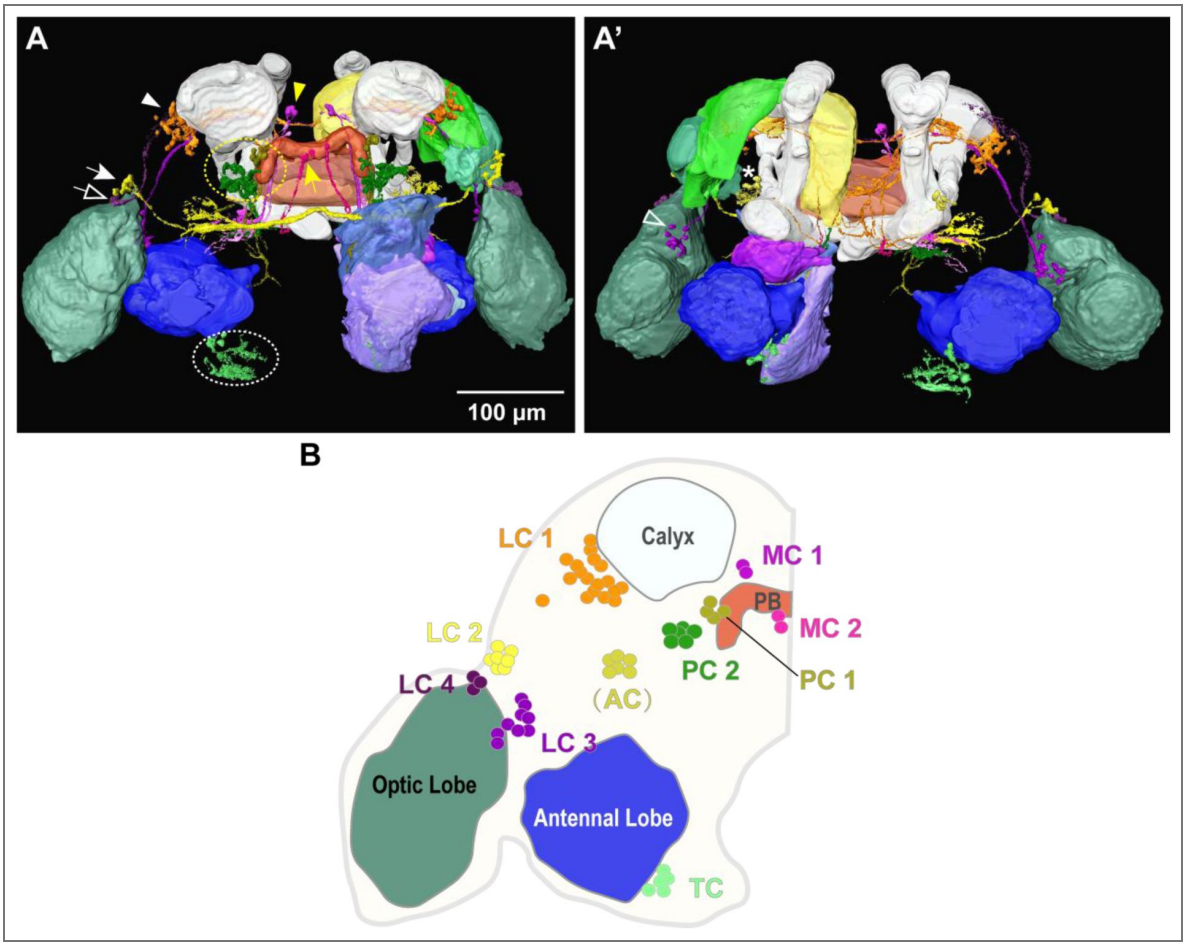

Figure 2. Overview on the reconstruction of the nine *Tc-foxQ2II* positive cell clusters.

(A) 3D reconstruction of major neuropils and EGFP-positive clusters of neurons based the brain shown in Fig. 1. Posterior view in (A) and anterior view in (A'). The cluster AC (white star in A') was not analyzed further as it was not Tc-foxQ2II positive. White circle: Tritocerebral cluster; yellow circle: Posterior cluster 1 and 2. (B) Schematic overview of the cell body locations for the ten clusters shown in the same colors as in A/A' and subsequent figures. White arrowhead: Lateral Cluster 1 (orange); white arrow: Lateral Cluster 2 (yellow); open arrowhead: Lateral Cluster 3 (purple); open arrow: Lateral Cluster 4 (dark purple); yellow arrowhead: Median Cluster 1 (magenta); yellow arrow: Median Cluster 2 (pink); yellow dashed circle: Posterior Cluster (PC1 is olive green and PC2 is vibrant green); white dashed circle: Tritocerebrum Cluster (light green and white broken circle in A); white star: Anterior Cluster (grass yellow). Scale bar: 100 μm.

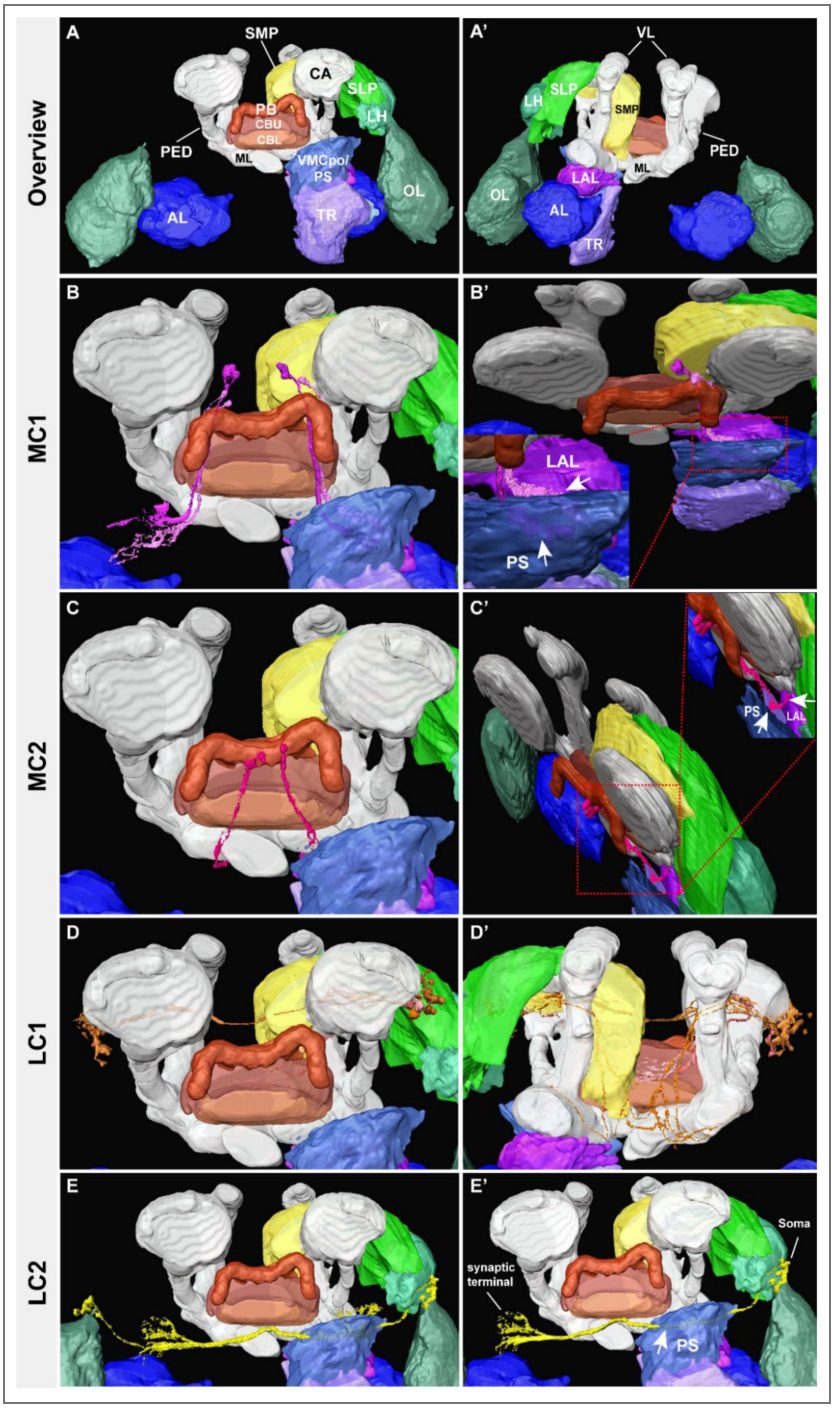

Figure 3. The morphology and distribution of EGFP-positive clusters.

(A-A') Posterior view and anterior views of the brain, showing major neuropils. (B-B') Median cluster 1 (MC1). (B) Posterior view. (B') Lateral view. The region enclosed by the red dashed square is magnified in the bottom-left corner, with a white arrow indicating the specific projection area. (C-C') Median cluster 2 (MC2). (C) Posterior view. (C') Lateral view. The central complex (CX) region, enclosed by a red dashed square, is magnified in the top-right corner. A white arrow indicates projections targeting the VMCpo/PS and LAL. (D-D') Lateral cluster 1 (LC1). (D) Posterior view. (D') Anterior view. (E-E') Posterior view of lateral cluster 2 (LC2). In (E'), a white arrow marks the VMCpo/PS region traversed by LC2. Abbreviations: AL: Antennal lobe; CB: Central body (CBU: Upper unit of the central body; CBL: Lower unit of the central body); LH: Lateral horn; MB: Mushroom body (CA: Calyx; ML: Medial lobe; PED: Peduncle; VL: Vertical lobe); OL: Optic lobe; PB: Protocerebral bridge; SLP: Superior lateral protocerebrum; SMP: Superior medial protocerebrum; TR: Tritocerebrum; VMCpo/PS: Ventromedial cerebrum postcommissural domain / Posterior slope.

projection of LC1a (orange in Fig. 5 A-A′) has two primary branches: one first circumvents the vertical lobe (VL, white) of the mushroom body (MB, white), then projects through the crepine toward the ventral region, and eventually arborizes in the ML (Fig. 5 A-A′). The other, LC1b (light coral in Fig. 5 B-B′), directly forms arborizations within the CB (white arrowhead in Fig. 5 A′). It does not circumvent the VL but projects through the superior lateral and medial protocerebrum directly between the VL and the peduncle (PED, white) of the MB, arborizing in the anterior surface of the CB (Fig. 5 B-B′).

Regarding the cell body location and the projections mainly to the mushroom body and the central complex (Supplementary Fig. 3 C-C'), LC1 cluster neurons appear similar to dopaminergic PPL1 cluster neurons in the *Drosophila* brain (see below for further data) (Mao and Davis, 2011; Hartenstein et al., 2017). The LC1a subcluster appears to innervate mainly the medial lobes of the mushroom bodies, similar to PPL101 dopaminergic neurons in *Drosophila* (Fig. 5 A′). Using immunohistochemistry, we confirmed dopamine expression in LC1a neurons that was expected for PPL1 neurons in *Drosophila* (see below). From the electron microscopy datasets (Scheffer et al., 2020; Schlegel et al., 2024) it appears that one at least one dopaminergic PPL1 neuron, PPL108 (Supplementary Fig. 3) displays an interconnection between the horizontal mushroom body lobes and the noduli of the central complex.

Lateral cluster 2-4 cells lie adjacent to the optic lobes and exhibit divergent projections

In LC2 (Fig. 3 E-E′), the cell bodies are located near the lateral horn (LH; mint green), with near-horizontal projections traversing the VMCpo/PS and ultimately projecting toward the VMCpo/PS of the opposite hemisphere. The cell bodies of LC3 (Fig. 4 A-A′) are located close to the optic lobe (OL; dark green), traverse the LH and the SLP, and arborize within the SMP (Fig. 4 A-A′). Based on the projection into the main neuropils and comparison with neurons in the *Drosophila* brain, LC3 is tentatively identified as a neuron similar to PPL2ab (Supplementary Fig. 3 E-E') (Farnworth et al., 2022; Mao and Davis, 2009). LC4 (Fig. 4 B-B′) projects from the OL, traverses the LH and arborizes in the SLP (indicated by white arrows in Fig. 4 B′). Taken together, the LC2-3 neurons have their cell bodies close to the optic lobes and project to the contralateral hemisphere without overt connectivity to MB or CX.

Note that due to the common origin of the four major projections from one large lateral cell cluster and due to the lack of single cell resolution in this analysis, the described assignments into LC1-4 subclusters remained tentative. We established and applied sparse marking of cells using the Brainbow system and added neurotransmitter analyses to confirm the interpretation (see below).

Posterior cluster cell bodies are located close to the PB but do not project into the central complex

The PC is subdivided into two subclusters based on the locations of cell bodies and their projections. The cell bodies of PC1 (Fig. 4 C-C′) are located adjacent to the lateral PB and project to the VMCpo/PS, forming Y-shaped arborizations in the VMCpo/PS of the central brain (red arrow in Fig. 4 C-C′). PC2 cell bodies are distributed in the inferior protocerebrum, central domain (IPc), located beneath the CA, and project to the VMCpo/PS and the LAL (Fig. 4 D-D′; white arrowhead marks cell bodies in D). Based on these characteristics, we hypothesize that the PC1 neurons may be homologous to the descending neurons (DNs) of *Drosophila* (Supplementary Fig. 3 F-F') (Namiki et al., 2018).

The Tritocerebrum Cluster

In the adult brain we found a cluster not described in He et al. and we named it TC (tritocerebrum cluster). The cell bodies of the TC are located between the antennal lobe (AL; blue) and the tritocerebrum (TR; light purple; Fig. 4E and white dashed circles in Fig. 1 A′-B′ and Fig. 2 A) and some projections are found within the TC (white arrow in Fig. 4 E). To check, whether the

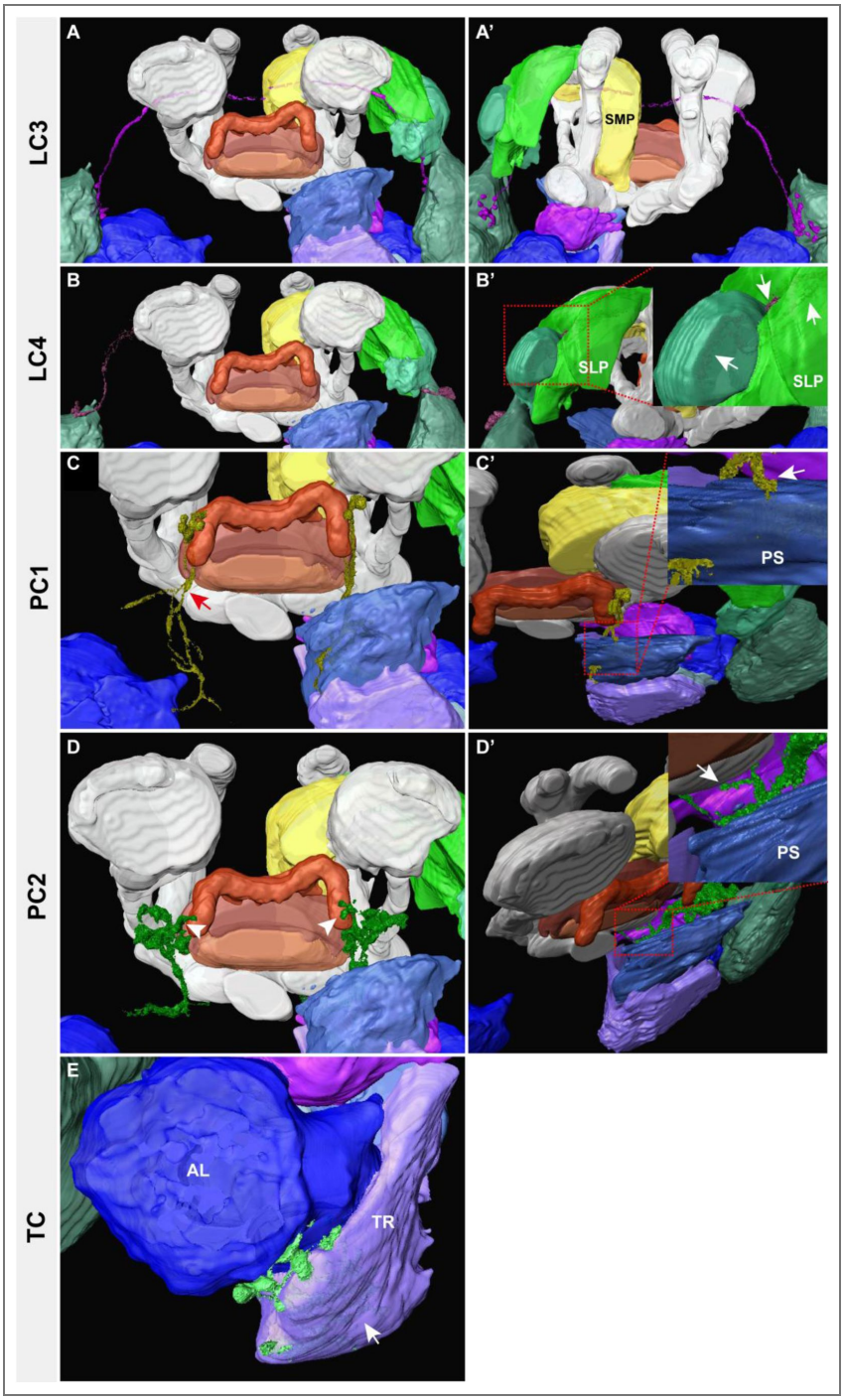

Figure 4. The morphology and distribution of EGFP-positive clusters in the brain of the *foxQ2-5' line*

(A- A') Lateral cluster 3 (LC3). (A) Posterior view. (A') Anterior view. (B-B') Lateral cluster 4 (LC4). (B) Posterior view. (B') Lateral view. A white arrow indicates LC4 arborization in the LH and SLP. (C-C') Posterior cluster 1 (PC1). (C) Posterior view. (C') Lateral view. The region enclosed by the red dashed square is magnified in the top-right corner. A white arrow shows where PC1 enters the VMCpo/PS. (D-D') Posterior cluster 2 (PC2). (D) Posterior view. (D') Lateral view. The projection region, enclosed by a red dashed square, is magnified in the top-right corner. A white arrow points to the arborization site. (E) Anterior view of tritocerebrum cluster (TC). A white arrow indicates its arborization zone. Abbreviations: AL: Antennal lobe; CB: Central body (CBU: Upper unit of the central body; CBL: Lower unit of the central body); LH: Lateral horn; MB: Mushroom body (CA: Calyx; ML: Medial lobe; PED: Peduncle; VL: Vertical lobe); OL: Optic lobe; PB: Protocerebral bridge; SLP: Superior lateral protocerebrum; SMP: Superior medial protocerebrum; TR: Tritocerebrum; VMCpo/PS: Ventromedial cerebrum postcommissural domain / Posterior slope.

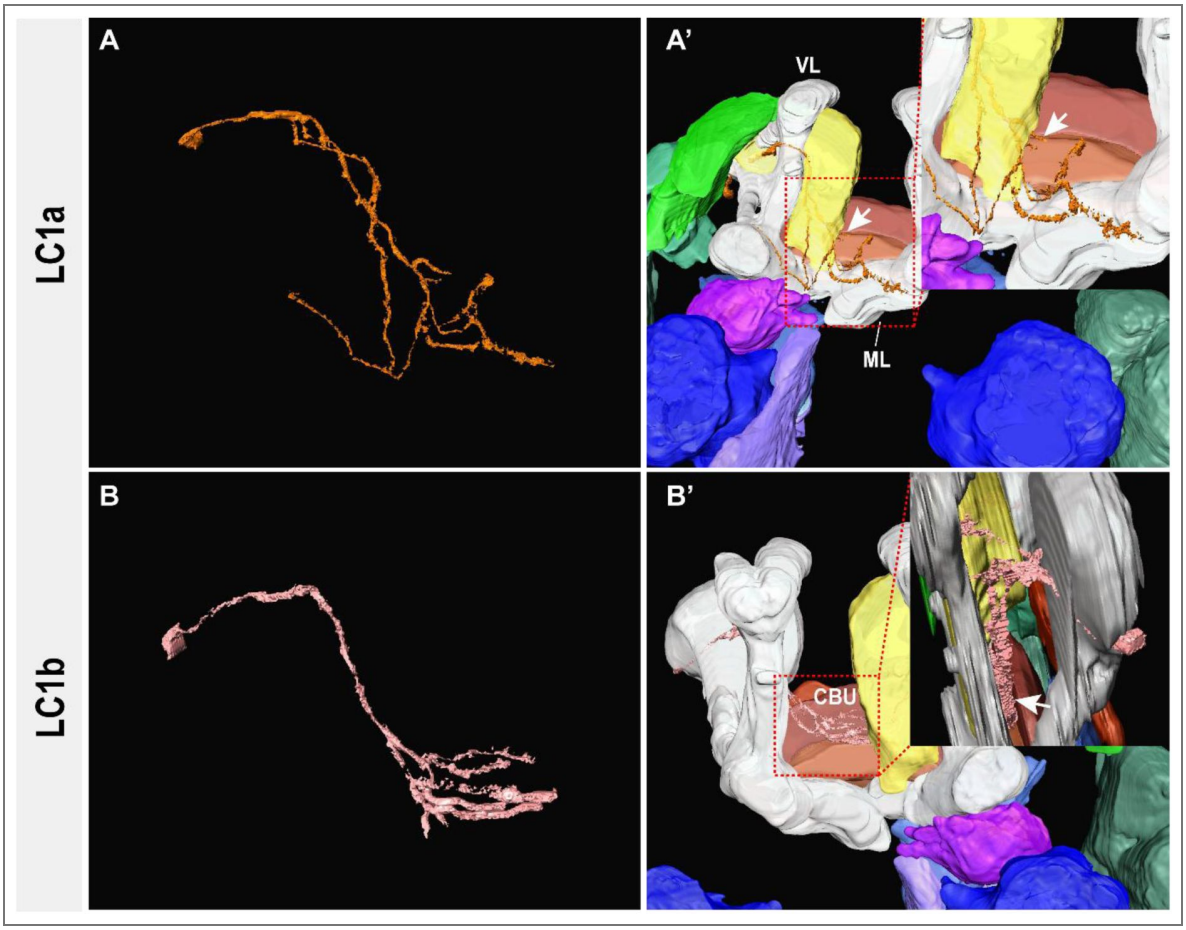

Figure 5. Classification of Lateral Cluster 1 based on distinct projection patterns.

(A-A') Morphology and projection pattern of LC1a, shown without (A) and with (A') brain compartments. The region enclosed by the red dashed square shows where LC1a passes near the central body (CB) before crossing the midline. A magnified view of this region (top-right corner) shows the LC1a projection adjacent to the CB, indicated by a white arrow. (B-B') LC1b projections. The boxed region in (B') shows that LC1b projects toward the CB. A magnified lateral view (top-right) details the contact point (white arrow). Abbreviations: VL: the vertical lobe; ML: the medial lobe; CBU: the upper unit of the central body.

TC emerges only during postembryonic development or had been overlooked previously, we did stainings in the L1 larval brain. Indeed, we found cells, which prefigure TC at that stage (white arrows in Supplementary Fig. 4).

In addition to the above described clusters, there were also cells whose projections could not be visualized or clearly tracked due to low signal (white arrows in Supplementary Fig. 5). In the absence of identifiable projections, we refrained from homologizing these cells.

Establishing the brainbow system in *Tribolium castaneum* for sparse marking of neurons

Due to the large number of marked neurons in the *foxQ2-5'-line* and the resulting overlapping projection patterns, it was difficult to unequivocally reconstruct the projection patterns of certain clusters (e.g. LC1). In order to test our hypotheses by an independent approach, we aimed at sparse labelling of *Tc-foxQ2II* positive neurons by establishing the Brainbow system in *Tribolium* (Livet et al., 2007). This was facilitated by the fact that the *foxQ2-5'-line* has a bicistronic transcription unit that codes for both, EGFP and the Cre-recombinase (Supplementary Fig. 6) (He et al., 2019). We generated a transgenic line with a Brainbow construct, which was adapted to *Tribolium* by using the endogenous EFA promoter (Sarrazin et al., 2012) and a modified combination of fluorescent proteins (mCherry, mEYFP and mCerulean; Supplementary Fig. 6A). By crossing this *Beetle-Brainbow-EFA line* with the *foxQ2-5'-line*, different fluorescent proteins were expected to be turned on randomly within the EGFP/Cre marked set of neurons. EYFP and Cerulean are derivatives of EGFP and are both recognized by the EGFP antibody, which was also used to mark all cells of our imaging line. Therefore, only the third fluorescent protein, mCherry, was scored by immunohistochemistry using an anti-RFP antibody. To test the system, we confirmed that mCherry expression from the *Beetle-Brainbow-EFA* line was dependent on the presence of the Cre construct (Supplementary Fig. 6 C). As the Cre recombinase activity increases with temperature (Buchholz et al., 1996), we tested the number of mCherry marked cells at two different temperatures, which reflect the upper and lower limits of the optimal living temperature of *Tribolium* (32 °C and 23 °C). In 20 brains grown at 23 °C, a total of 79 cells were marked (Supplementary Fig. 7). Some clusters were frequently marked with several cells, while others were marked much more rarely. The six brains grown at 32 °C showed no clear increase in the number of marked cells (Supplementary Fig. 7). As a comparably large number of cells were marked in each brain, the projections of the neurons of interest often converged with those of other neurons, which made unequivocal reconstruction of the entire projection pattern of the neurons impossible. In summary, the system allows for sparse random marking of cells but does not provide single cell resolution.

Confirming cluster assignments using the *Tribolium brainbow* system

After mating the *foxQ2-5'-line* with the *Beetle-Brainbow-EFA line*, we collected brains from the offspring (grown at 23°C) and stained for mCherry. From 20 brains we reconstructed in total 79 single marked neurons or small neural clusters. For conservative analysis, we selected cells that had no or comparably few marked neighbors and reconstructed only the main projections as far as they were unequivocal. We were able to confirm all clusters described above except for LC3 (Fig. 6).

Two subclusters had tentatively been assigned to LC1 (Fig. 5) and we used sparse Brainbow labeling to further test this hypothesis. We found that 10 cells from 9 brains reflected the LC1 projection pattern (Supplementary Fig. 8). After segmentation of these cells, we confirmed the presence of two subclusters LC1a and LC1b based on the fact that some neurons passed anterior of the vertical lobe of the MB (LC1a, Fig. 5A') while others projected posterior to it into the central brain (LC1b, Fig. 5B'). Each was confirmed by 5 neurons, respectively (Supplementary Fig. 8).

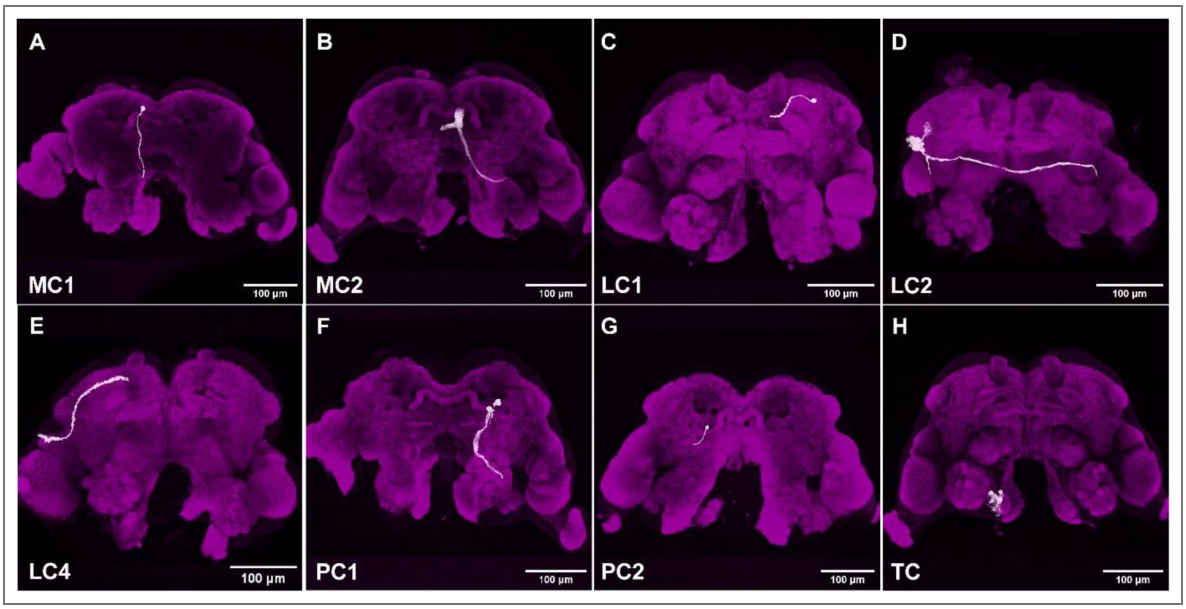

Figure 6. Eight clusters detected in the *foxQ2-5′– line* were also sparsely labelled by Brainbow.

(A) MC1. (B) MC2. (C) LC1. (D) LC2. (E) LC4. (F) PC1. (G) PC2. (H) TC. All panels show the brain of the *foxQ2-5′- line*. Magenta represents synapsin. Scale bar: 100 µm.

Embryonic expression of *Tc-foxQ2II* is not maintained in all daughter cells

The *foxQ2-5'-line* is an enhancer trap reflecting the current state of expression of *Tc-foxQ2*. In brainbow, in contrast, expression continues permanently once turned on by recombination. Therefore, discrepancy in the patterns can be observed if cells had turned on brainbow e.g. during embryonic *Tc-foxQ2II* expression but subsequently ceased to express Tc-foxQ2. Such cases would be detectable by observing mCherry projections in the adult brain, which were not found in the *foxQ2-5'-line*. Indeed, we observed Brainbow marked neurons in the adult brain, which had not been observed in the *foxQ2-5'-line* (Supplementary Fig. 9 and 10). Notably, columnar neurons were observed among these cells, connecting distinct neuropils of the central complex (CX) and other brain structures through four prominent tracts (termed the WXYZ tracts) (Supplementary Fig. 9 A). This marking was dependent on Cre from the *foxQ2-5'-line* because the *Beetle-Brainbow-EFA line* alone showed no mCherry signal (Supplementary Fig. 6 C). We conclude that these cells had expressed *EGFP/Cre* for some time during development but had shut down expression at later stages. The marking of columnar neurons is in line with the embryonic expression of *Tc-foxQ2II* in Type II neural lineages (He et al., 2019). In summary, during development, *Tc-foxQ2II* expression seems to be shut down in subsets of neurons. It is noteworthy that some columnar neurons stem from early *Tc-foxQ2II* positive cells while ongoing *Tc-foxQ2II* expression marks no columnar cells but some tangential cells of the CX (among other types of cells).

LC1a interneurons innervate the *mushroom body* and the *central complex*

In our imaging line, we found plenty arborizations within the MBs and the CX (Fig. 7; arrows in Fig. A' and arrowhead in Fig. B' and single optical sections cutting through these neuropils in Fig. 7A" and B"). Specifically, LC1 seems to comprise cells strongly innervating the MB and/or CX. The projections of LC1a (Fig. 5A) appear to arborize in the mushroom body medial lobes similar to the projection pattern of the LC1a neurons from the dopaminergic PPL1 cluster in adult *Drosophila* that have been identified as PPL101 in the electron microscopy dataset (Scheffer et al., 2020; Schlegel et al., 2024) (Fig. 5 A').

We wondered, whether single neurons would innervate both, MB and CX but the resolution of our standard LSM images did not allow separating the neurites clearly. To characterize the projections of these neurons more in detail, we performed STED high resolution microscopy of that region (Willig et al., 2006) and performed a more precise reconstruction of neurons belonging to the two subclusters of LC1 (Fig. 8A-B and Supplementary Fig. 18). LC1 neurons arborize in both the upper unit of the central body (CBU) and the medial lobe of the mushroom body (Fig. 8 A and Supplementary Fig. 18). In the CBU, they arborize extensively (yellow in Fig. 8C-F) while the tracts continue to the contralateral side meeting the other LC1 tracts at the midline (white in Fig. 8C-F). While the resolution of the STED images was clearly better (Supplementary Fig. 19) it did not suffice to unequivocally show or rule out that there are LC1 cluster neurons, which innervate both, MB and CX. This hypothesis will have to to be tested by enhanced tools for single cell marking (as opposed to sparse marking of our brainbow system). We note that there are EGFP-marked projections also in other parts of the MBs and the crepine (e.g. Fig. 7A" and B"). Due to the dense labelling of *Tc-foxQ2II* positive neurons these could not be assigned unequivocally to certain neurons but they all seemed to be dopaminergic.

Neurotransmitter content of *Tc-foxQ2II* positive cells

To better characterize the neuron subtypes within *Tc-foxQ2II* positive clusters, we examined the expression of six major neurotransmitters (Lacin et al. 2019). Neither GABA nor serotonin (5-HT) were expressed in neurons marked by EGFP (Table 1 and Supplementary Fig. 11 and 12). Most adult *Tc-foxQ2II* neurons were positive for the fast-activating neurotransmitters acetylcholine (visualized by immunohistochemistry targeting Choline Acetyltransferase (ChAT)) and Glutamate (Supplementary Fig. 13 and 14). This suggests that the *Tc-foxQ2II* cells contribute to fast neural circuits in the central nervous system (CNS). We found these neurotransmitters expressed in the MB and CX as well (Supplementary Fig. 15 A and B).

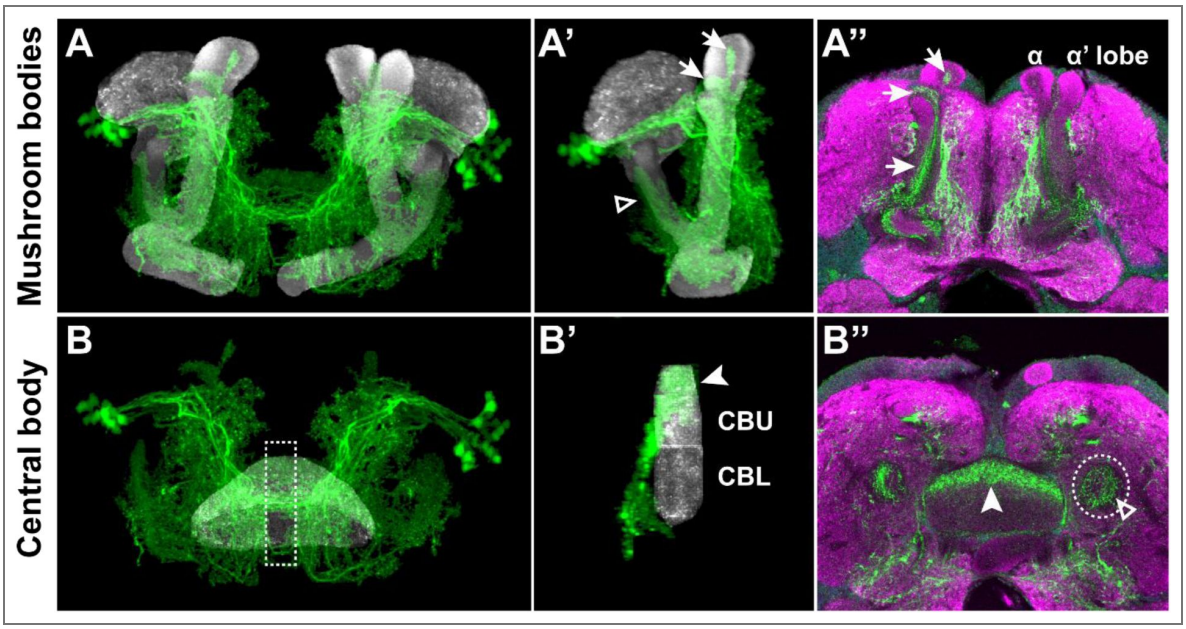

Figure 7. EGFP-positive cells arborize in the mushroom body and the central complex.

(A-A'') Arborizations of EGFP-positive cells in the mushroom body (MB). (A) Overview of 3D reconstruction of the MB and EGFP-positive projections, generated using VVDviewer. (A') Hemi-mushroom body with EGFP-positive projections. (A") Immunohistochemistry result showing the MB and EGFP-positive projections. White arrows in (A') and (A'') indicate EGFP-positive projections arborizing in the α and α' lobe of the MB. (B-B'') Arborizations of EGFP-positive cells in the central body (CB). (B) Overview of the 3D reconstruction of the CB with EGFP-positive projections. (B') Side profile view of the area marked by the white dashed rectangle in (B). (B'') Immunohistochemistry result showing the CB and EGFP-positive projections. White arrowheads in (B') and (B'') indicate EGFP-positive projections arborizing in the upper unit of the central body (CBU). Open arrowheads in (A') and (B'') indicate the EGFP-positive projections arborizing in the peduncle (PED). The White dashed circle in (B'') outlines the PED. Green, EGFP; magenta, synapsin; and white, neuropils (MB or CB).

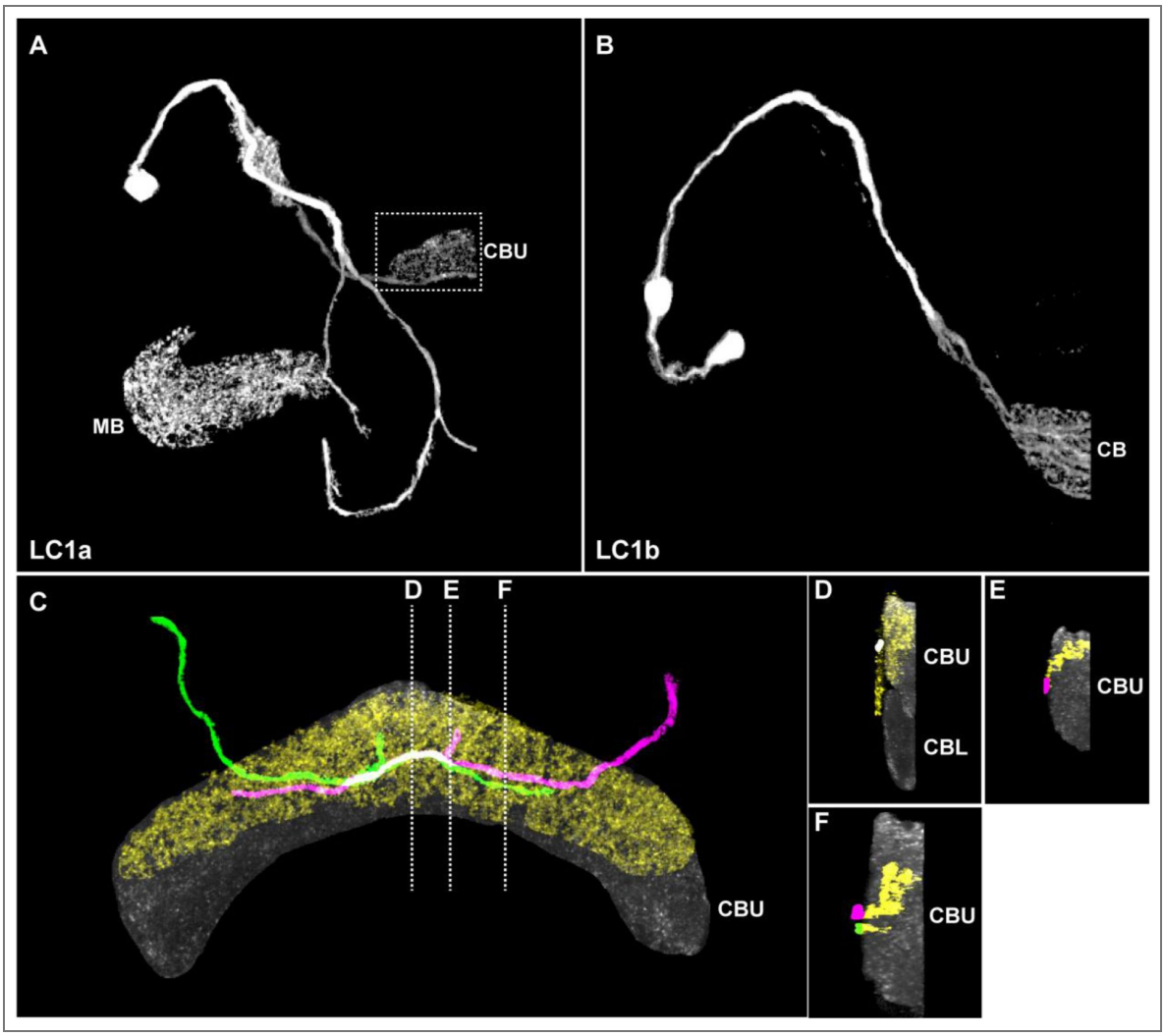

Figure 8. Reconstruction of STED-imaging of LC1a connection of mushroom body with the central complex in the *foxQ2-5′- line* brain.

(A) LC1a seems to have two main branches: one innervates the mushroom body (MB), and the other innervates the upper unit of the central body (CBU). (B) LC1b arborizes only within the central body (CB). (C) A higher-magnification view of the projections in the CBU (region partially outlined by the white dashed rectangle in A). (D-F) Transverse sections through distinct domains of the central body. (D) Median section. (E) A lateral section showing a single branch projecting into the CB. (F) A section where two distinct tracts are visible. Green and magenta represent the main projections from different sides, which are in close proximity around the midline (white). Yellow indicates arborizations within the CBU. CBU is shown in grey. CBL: lower unit of the central body. The STED dataset used in this panel was acquired by Ying.

Neurotransmitters	Types of EGFP-positive cells in the *foxQ2-5′-line*								
	MC1	MC2	LC1	LC2	LC3	LC4	PC1	PC2	TC
Acetylcholine (ChAT)									
Glutamate									
Dopamine (TH)									
Octopamine (TBH)									
GABA									
Serotonin (5-HT)									

(Color code: grey, positive; white, negative.)

Table 1. Neurotransmitter expression in different EGFP-positive cell types in the *foxQ2-5′-line* brain

Grey indicates clusters that contained at least one neuron expressing the respective transmitter. Hence, it does not mean that all cells of a cluster have a respective transmitter nor that transmitters are co-expressed in the neurons.

Five clusters included cells positive for the biogenic amines dopamine (detected by expression of TH, Tyrosine Hydroxylase) and octopamine (detected by TBH, Tyramin-β-Hydroxylase) (Table 1; Fig. 9 and 10, and Supplementary Fig. 16). Dopamine was found in projections within the MB and CX (Supplementary Fig. 15 C-C') while TBH stained only the cell somata (data not shown).

Biogenic amines are involved in learning and memory and setting arousal threshholds (Davis, 2023), which are functions performed by the *mushroom bodies* and related to the function of the *central complex* in goal directed navigation, respectively. Therefore, we focused on the analysis of dopamine in the *Tc-foxQ2II* positive neurons. First, we determined the number of cells within each cluster that were dopamine-positive and calculated the overlap ratio for each cluster (Fig. 10 A-F). In the MC (the counts for MC1 and MC2 were aggregated), overall, 76.0% of Tc-foxQ2II neurons express dopamine (Fig. 10 A-A'' and F). In the LC1, the overlap ratio between dopamine-positive and FoxQ2-positive neurons was 58.3% (Fig. 10 B-B'' and F) in the LC2 it was 63.5% (Fig. 10 C-C'' and F) and in LC3 87.0% (Fig. 10 D-D'' and F). In summary, across these clusters 60-90 % of the FoxQ2 neurons were dopamine-positive. On the other hand, we sought to determine the proportion of dopaminergic neurons that express FoxQ2. By quantifying the total number of dopamine-positive cells in the brain (excluding the optic lobe) relative to those that are also FoxQ2-positive, we found that 25.8% of dopaminergic neurons were FoxQ2-positive (n = 5).

Octopamine-labeled neurons were found in the same clusters as dopamine. For instance, octopamine staining was observed in some cells within the median cluster (MC1 and MC2) and the lateral clusters (LC1, LC2, and LC3) (Table. 1 and Supplementary Fig. 16). The portion of cells positive for octopamine within the clusters (MC, LC1, LC2 and LC3) was 61.5%, 45.2%, 58.1%, and 62.1%, respectively (Supplementary Fig. 16 H). Hence, octopamine is expressed in fewer cells compared to dopamine.

FoxQ2 positive dopaminergic neurons can be assigned to fly neuron types and allow confirming clusters

Because only a subset of *Tc-foxQ2II* neurons are dopaminergic, we utilized TH staining as an alternative way for sparse marking. This allowed the reconstruction of clusters with greater clarity (Fig. 11 A and Supplementary Fig. 17). Analyzing the TH/EGFP double positive neurons confirmed the assignment of clusters outlined above (Compare Fig. 11 with Fig. 3 and 4). Specifically, we confirmed that the MC-cells do not cross the midline but project towards lateral regions (Fig. 11 B) and that the dopamine-positive neurons in MC1 strongly resemble PPM1 cluster dopaminergic neurons. Clusters LC2 (yellow in Fig. 11 A, E) and LC3 (green in Fig. 11 A, E) were confirmed, as well. Based on neurotransmitter content, neuronal morphology and comparison with the *Drosophila* database, we hypothesize that the dopamine-positive neurons in LC2 may correspond to PPL2c, that show similarities with the neuron with the identity CB0452 in the electron microscopy dataset (Schlegel et al., 2024), that recently has been predicted as being dopaminergic (Eckstein et al., 2024) and those in LC3 may correspond to PPL2ab (Supplementary Fig. 3) that have been identified as PPL204 in the electron microscopy dataset (Scheffer et al., 2020; Schlegel et al., 2024).

With respect to the connection between MB and CX we found that all dopamine-positive cells from LC1 projected towards the CB contacting the MB on their way (Fig. 11 C-D'''). Furthermore, we identified the previously detected LC1a and LC1b subtypes (Fig. 11 D-D''' ; compare to Fig. 5). The neurons potentially connecting CB with MB were dopamine positive and similar to the *Drosophila* PPL1 subtype.

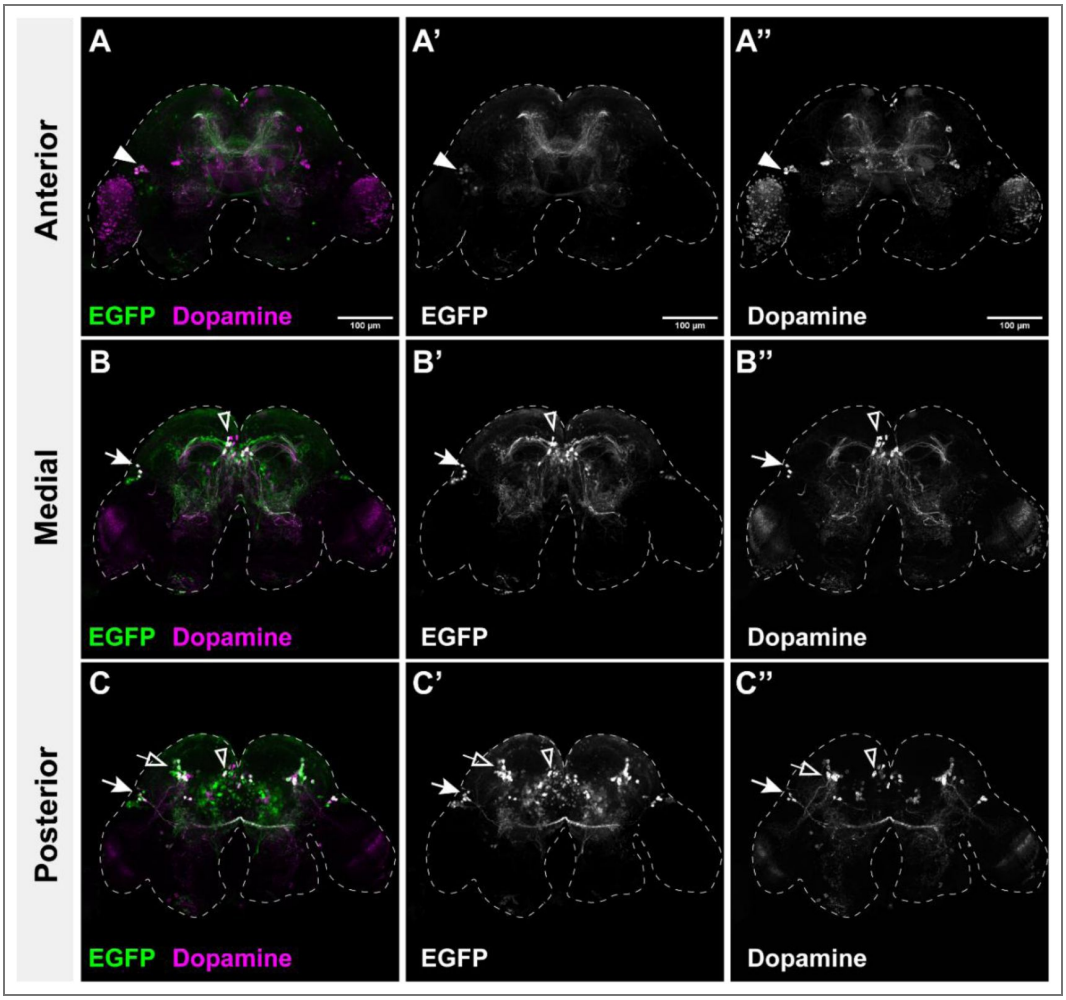

Figure 9. A subset of Tc-FoxQ2-positive neurons are dopaminergic.

Co-immunostaining for GFP (green) and the dopamine marker Tyrosine Hydroxylase (TH, magenta) identifies dopaminergic subtypes among the Tc-FoxQ2-positive neuronal populations. Dashed outlines indicate the brain contour. (A-A'') The anterior brain region containing lateral cluster 3 (LC3, white arrowheads). (A') GFP channel. (A'') TH (dopamine) channel. (B-B'') A medial section showing the median cluster (MC, open arrowheads), and lateral cluster 2 (LC2, white arrows). (C-C'') A posterior section showing the median cluster (MC, open arrowheads), lateral cluster 1 (LC1, open arrows) and lateral cluster 2 (LC2, white arrows). Scale bar: 100 µm.

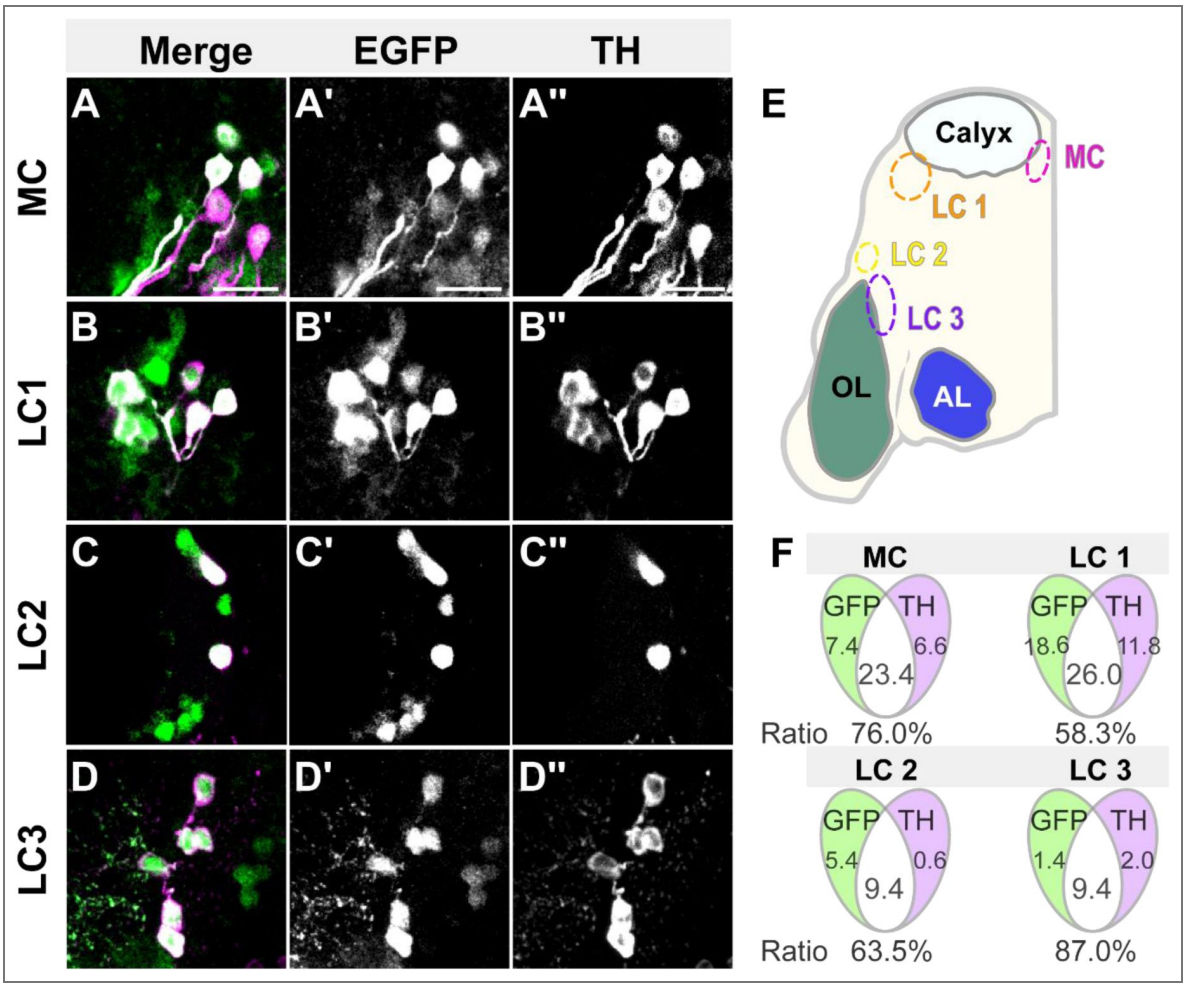

Figure 10. Co-expression of Tc-foxQ2II and TH (dopamine) in distinct neuronal subsets.

A magnified view highlights neuronal subtypes co-expressing the dopaminergic marker Tyrosine Hydroxylase (TH) and Tc-FoxQ2/EGFP, alongside an analysis of the signal overlap ratio. (A-D'') A representative imaging plane showing co-immunostaining for neurons expressing both EGFP (green) and TH (magenta). (E) Schematic of the left-brain hemisphere. Four Tc-FoxQ2-positive neuronal subtypes are outlined with differently colored dashed circles. (F) Venn diagrams quantify the overlap between TH-positive and Tc-FoxQ2-positive neurons for each of the four subtypes (n = 5). Scale bar: 20 μm.

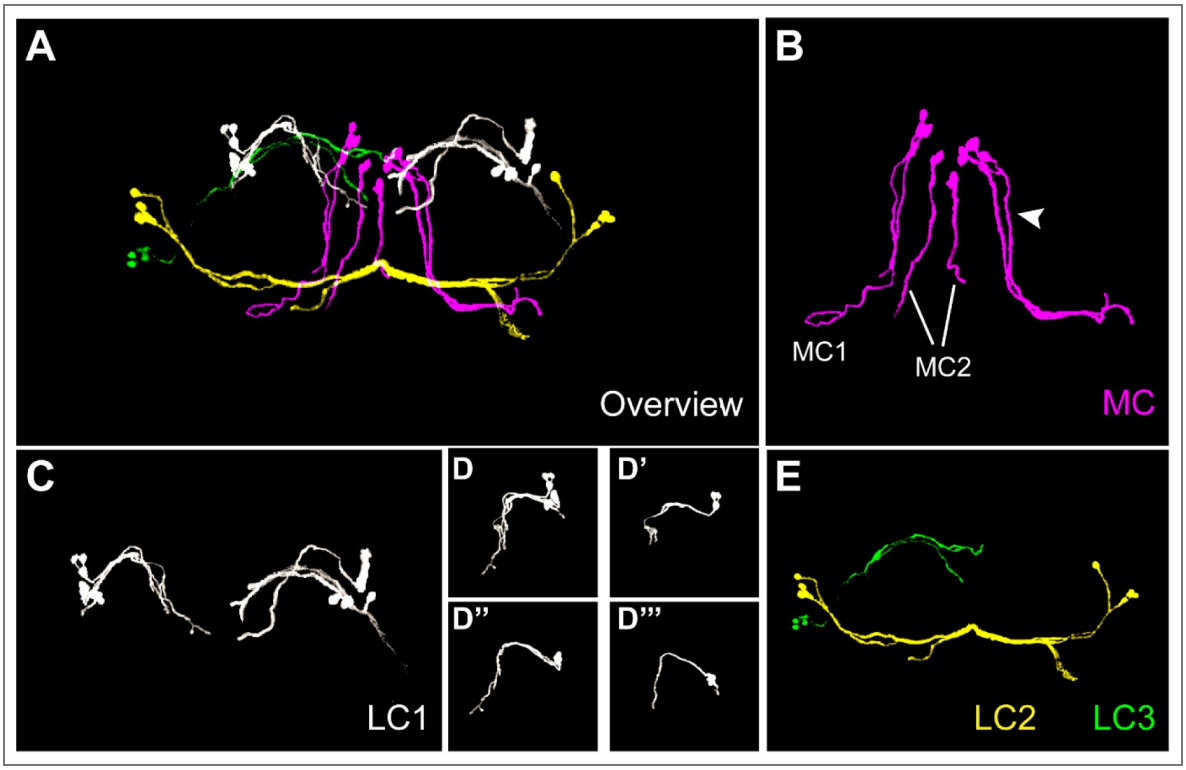

Figure 11. 3D reconstruction of *Tc-foxQ2*-Dopaminergic neuronal projections in the brain of *foxQ2-5'-line* using VVDviewer.

(A) Overview of the projections from the four neuronal subtypes. (B) Projections from the median cluster (MC). MC1 contains two long tracts (indicated by a white arrowhead), consistent with previous descriptions. (C) Projections from all subtypes within lateral cluster 1 (LC1). (D-D''') Individual projections of each LC1 subtype. (D) Overview of the hemi-LC1. (D') LC1a projection (see also Fig. 5). (D''-D''') LC1b projections (see also Fig. 5). (E) Projections from LC2 and LC3.

Discussion

Tc-foxQ2II is expressed in fast-acting neurons and may be involved in the specification of subtypes of dopaminergic neurons

foxQ2II is an ancestral transcription factor involved in anterior patterning of most animal clades but notably was lost from vertebrates. Given its documented role in apical organ development, it is likely involved in specifying sensory and neuroendocrine cells. Indeed, other paralogs of that family have been shown to be involved in sensory cells of the cnidarian apical organ and the fish retina (Gattoni et al., 2025b; Ogawa et al., 2021). However, the contribution of *foxQ2II* marked neurons to the adult brain has remained unstudied. Therefore, our results give a first impression of *foxQ2II* function in protostome brains and provides a basis for comparison with deuterostomes. We found a wide range of different neuron types to be marked by *Tc-foxQ2II*. Nine clusters of neurons were distinguished by cell body location and projection pattern. Cell body locations ranged from median-anterior to posterior-lateral, arborizations innervated different neuropils and both ipsilateral and contralateral projections were found. Hence, neurons marked by this transcription factor have not much morphological similarity. Intriguingly, a pattern was found with respect to the neurotransmitters: Adult *Tc-foxQ2II* positive neurons seem to be predominantly fast acting as most of them express Glutamate and/or the marker for cholinergic neurons (ChAT). None of the neurons was positive for serotonin (5-HT) or GABA. The former function corresponds to studies of foxQ2 in sea urchin, where serotonergic neurons develop in a region that has lost foxQ2 expression (Yaguchi et al., 2016). Interestingly, only a subset of dopaminergic neurons was *Tc-foxQ2II* positive in *Tribolium*. We therefore hypothesize that it may be involved in the specification of dopaminergic neuron subtypes. The fact that not all dopaminergic neurons were *Tc-foxQ2II* positive and that only parts of the *Tc-foxQ2II* marked cells of any given cluster was dopamine positive indicates additional regulation, e.g. by other transcription factors and/or the Delta Notch pathway, which defines two divergent hemilineages from one neural lineage (Truman et al., 2010). Taken together, *Tc-foxQ2II* is likely part of the combinatorial specification system of adult neurons, where transcription factor “cocktails” determine cell identity. This paradigm of neural specification has been established in the insect ventral nerve cord (Skeath and Thor, 2003; Technau et al., 2006) and is thought to act in the brain as well, albeit involving different genes (Epiney et al., 2025; Özel et al., 2022; Urbach et al., 2003). To disentangle the precise regulatory function, it will be required to mark individual or small subsets of *Tc-foxQ2II* positive neurons before performing functional tests with candidate regulators.

Stage specific expression of *Tc-foxQ2II* in columnar and tangential neurons of the central complex

The central complex (CX) is a highly complex neural structure composed of very distinct types of neurons. Among them is the class of columnar neurons, which have their cell bodies in the *pars intercerebralis* and interconnect slices of different CX subdivisions in a complex but largely conserved projection pattern. Tangential neurons in contrast connect other brain regions to certain CX subdivisions (Pfeiffer and Homberg, 2014). It came as a surprise that *Tc-foxQ2II* seems to be active in lineages giving rise to both, columnar and tangential neurons. Specifically, the *foxQ2-5’* enhancer trap activity indicated ongoing expression in the adult brain of *Tc-foxQ2II* in tangential (but not columnar) neurons of the CX. In contrast, the permanent marking by the brainbow system revealed columnar neurons as well (Supplementary Fig. 9). This indicates that the enhancer trap line had been active in neural lineages that give rise to columnar neurons at early stages but that *Tc-foxQ2II* expression was shut down in the adult brain. In line with this hypothesis, we have detected embryonic *Tc-foxQ2II* expression in putative type II neuroblasts, which are known to contribute to columnar neurons (He et al., 2019). Hence, the same transcription factor can be involved in the development of fundamentally different neuron types of one brain center such as columnar and tangential neurons. Temporally separated activity in the

different lineages may be required for that multifaceted role. Interestingly, the transcription factor *retinal homeobox* also marks both, columnar and tangential neurons in *Tribolium* and *Drosophila* (Bullinger, 2024). Hence, this pattern might be more widespread and reflect a developmental principle.

FoxQ2II marks dopaminergic neurons of the higher brain centers *mushroom bodies* and *central complex*

The mushroom bodies (MBs) and the CX are two higher order brain centers with functions in learning and memory and spatial orientation, respectively (Heisenberg, 2003; Pfeiffer and Homberg, 2014). Only recently, connections between these two neuropils were found in flies based on EM connectome and transsynaptic tracing. Specifically, some mushroom body output neurons (MBONs) seem to connect to the fan-shaped body (Kandimalla et al., 2023; Li et al., 2020; Scaplen et al., 2020) and there is evidence for such connections in *Heliconus* butterflies as well (Farnworth et al., 2025). With respect to dopaminergic neurons, in the electron microscopy dataset it appears that the PPL108 neuron was found to connect the noduli of the CX with the MBs(Scheffer et al., 2020; Schlegel et al., 2024). We find that *Tc-foxQ2II* is expressed in some dopamine positive PPL1 neurons. Our reconstructions indicate that some of these neurons have arborizations in the MBs and the fan-shaped body of the CX. We cannot rule out that there are *Tc-foxQ2II* positive dopaminergic neurons from this cluster that provide direct connectivity between these brain centers. For the time being, this has to remain a hypothesis because too many neurons were marked to make clear statements. A transgenic system to mark single cells in *Tribolium* will be required to unequivocally show such neurons. Our brainbow approach allowed for sparse marking but did not reach single cell resolution. Localizing the fluorescent proteins to the membrane for better resolution (Karapidaki et al., 2025), increasing the expression level for sensitivity and reducing the efficacy of Cre-recombination are steps that would enhance the system.

3.1.6 Materials and methods

Animals

Tribolium castaneum stocks were raised under standard conditions at 32 °C or 23 °C. The *foxQ2-5'-line* (He, 2019), an enhancer trap transgenic line generated by genome editing, was used for immunohistochemical staining, behavioral testing and RNAi experiments. The *Beetle-Brainbow-EFA line* (generated using the strategy described in (Schomburg, 2010)) was used for sparse labeling of *Tc-foxQ2II* positive cells.

Immunohistochemistry

Immunohistochemistry of larval and adult brains was performed according to a previously described protocol (Hunnekuhl VS et al., 2020). The following primary antibodies were used: chicken anti-GFP (1:2000, Abcam plc; RRID: ab13970), rabbit anti-GFP (1:1000, Thermo Fisher Scientific Inc.; RRID: A-11122), rabbit anti-RFP (1:1000, Abcam; *RRID:AB_945213*), guinea pig anti-FoxQ2 (1:1000) (He, 2019), mouse anti-Synapsin (1:25, DSHB; RRID: 3C11), mouse anti-Tyrosine-Hydroxylase (1:1000, Immunostar Inc.; RRID: 22941), rabbit anti-Serotonin (1:1000, Sigma-Aldrich, Merck KGaA; RRID: S5545), rabbit anti-GABA (1:100, Sigma-Aldrich, Merck KGaA; RRID: A2052), mouse anti-Glutamate (1:1000, Sigma-Aldrich; RRID: G9282), mouse anti-ChAT4B1 (1:200, Developmental Studies Hybridoma Bank; *RRID:AB_528122*) and rabbit anti-TβH (1:30, a gift from Uwe Homberg). Secondary antibodies coupled with Alexa Fluor 488, Alexa Fluor 555 or Alexa Fluor 647 (Thermo Fisher Scientific, RRID: A-11039, RRID: A-11070, RRID: A-21435, RRID: A-21425, RRID: A-21430, RRID: A-21450, RRID: A-21235, RRID: A-21245) were used at 1:1000. STED imaging was performed with the following secondary antibodies: Goat anti-rabbit STAR RED (1:1000, Abberior, RRID: STRED-1002-500UG) and Goat anti-mouse STAR ORANGE (1:1000, Abberior, RRID: STORANGE-1001-500UG). DAPI (1:2000, Thermo Fisher Scientific Inc.; RRID: D1306) was used to stain nuclei.

Cell counting

To quantify the number of cells in each cluster, we used the Cell counter plugin in FIJI to manually count somata of neurons in confocal image stacks of the brains analyzed in this study. Cells of interest were identified based on EGFP, mCherry or dopamine (TH) signals. Different clusters were distinguished according to cell position and projection patterns. Cell counts were performed on five standard brains.

3D reconstruction

The neuropil compartments of the adult brain were reconstructed using Amira software (Thermo Fisher Scientific), based on synapsin immunostaining and following the morphological framework described by Farnworth (Farnworth et al., 2022). Neuronal projections were reconstructed from confocal image stacks using VVD software (Lillvis et al., 2022).

Image processing and documentation

Immunohistochemical samples were imaged using a Zeiss LSM 980 confocal laser scanning microscope to generate multichannel image stacks. Each stack, with a resolution of 1024 × 1024 pixels, contained 100-200 slices depending on the specimen. Stacks were processed and analyzed using FIJI (Schindelin et al., 2012), with brightness and contrast adjusted as needed. Final figures were assembled in Adobe Illustrator 2020 (Adobe). The original image stacks are available in both TIF and AVI formats on Figshare (*https://figshare.com/s/379a7896e38863e07aa7*).

Data availability

The original LSM stacks and respective videos of the specimen shown in the figures are available on FigShare *https://figshare.com/s/379a7896e38863e07aa7*. The sequence of the Brainbow construct is given in the supplementary. The transgenic stocks are kept in and are available from the Bucher lab.

Acknowledgements

We thank Uwe Homberg for kindly providing the rabbit anti-TβH antibody. STED-compatible secondary antibodies, goat anti-rabbit STAR RED and goat anti-mouse STAR ORANGE, were obtained from Abberior. We thank Dawid Lbik for pointing out the potential of STED imaging and we acknowledge the technical support by Marita Buescher, Elke Küster and Claudia Hinners.

Additional information

Funding

Funder	Grant reference number	Author
China Scholarship Council (CSC)	202104910052	Ying Pang
Deutsche Forschungsgemeinschaft (DFG)	BU1443/17-1	Gregor Bucher

Author ORCID iDs

Michalis Averof: https://orcid.org/0000-0002-6803-7251
Thomas Riemensperger: https://orcid.org/0000-0002-5872-7398
Gregor Bucher: https://orcid.org/0000-0002-4615-6401

References

Bellen HJ, Tong C, Tsuda H (2010) 100 years of Drosophila research and its impact on vertebrate neuroscience: a history lesson for the future. *Nat. Rev. Neurosci* **11**:514-522 https://doi.org/10.1038/nrn2839 | PubMed

Bello BC, Izergina N, Caussinus E, Reichert H (2008) Amplification of neural stem cell proliferation by intermediate progenitor cells in Drosophila brain development. *Neural Develop* **3**:5 https://doi.org/10.1186/1749-8104-3-5 | PubMed

Boone JQ, Doe CQ (2008) Identification of Drosophila type II neuroblast lineages containing transit amplifying ganglion mother cells. *Dev. Neurobiol* **68**:1185-1195 https://doi.org/10.1002/dneu.20648 | PubMed

Boyan G, Williams L, Legl A, Herbert Z (2010) Proliferative cell types in embryonic lineages of the central complex of the grasshopper Schistocerca gregaria. *Cell Tissue Res* **341**:259-277 https://doi.org/10.1007/s00441-010-0992-6 | PubMed

Buchholz F, Ringrose Leonie, Angrand Pierre-Olivier, Rossi Fabio, Francis Stewart A (1996) Different thermostabilities of FLP and Cre recombinases: implications for applied site-specific recombination. *Nucleic Acids Res* **24**:4256-4262 https://doi.org/10.1093/nar/24.21.4256 | PubMed

Bullinger GC (2024) Conservation and divergence of the retinal homeobox genetic neural lineage between Drosophila melanogaster and Tribolium castaneum. Göttingen University.

Busengdal H, Rentzsch F (2017) Unipotent progenitors contribute to the generation of sensory cell types in the nervous system of the cnidarian Nematostella vectensis. *Dev. Biol* **431**:59-68 https://doi.org/10.1016/j.ydbio.2017.08.021 | PubMed

Davis RL (2023) Learning and memory using Drosophila melanogaster: a focus on advances made in the fifth decade of research. *Genetics* **224**:iyad085 https://doi.org/10.1093/genetics/iyad085 | PubMed

Eckstein N, Bates AS, Champion A, Du M, Yin Y, Schlegel P, Lu AK.-Y, Rymer T, Finley-May S, Paterson T, *et al.* (2024) Neurotransmitter classification from electron microscopy images at synaptic sites in Drosophila melanogaster. *Cell* **187**:2574-2594. https://doi.org/10.1016/j.cell.2024.03.016 | PubMed

Epiney D, Chaya GNM, Dillon NR, Lai S.-L, Doe CQ (2025) Transcriptional complexity in the insect central complex: single nuclei RNA-sequencing of adult brain neurons derived from type 2 neuroblasts. *bioRxiv* https://doi.org/10.1101/2023.12.10.571022

Farnworth MS, Eckermann KN, Bucher G (2020) Sequence heterochrony led to a gain of functionality in an immature stage of the central complex: A fly–beetle insight. *PLOS Biol* **18**:e3000881 https://doi.org/10.1371/journal.pbio.3000881 | PubMed

Farnworth MS, Bucher G, Hartenstein V (2022) An atlas of the developing *Tribolium castaneum* brain reveals conservation in anatomy and divergence in timing to *Drosophila melanogaster*. *J. Comp. Neurol* **530**:2335-2371 https://doi.org/10.1002/cne.25335 | PubMed

Farnworth MS, Toh YP, Loupasaki T, Hodge EA, Jundi B. el, Montgomery SH (2025) Distinct evolutionary trajectories of two integration centres, the central complex and mushroom bodies, across Heliconiini butterflies. *eLife* **14**:RP107589 https://doi.org/10.7554/eLife.107589

Gattoni G, Keitley D, Sawle A, Benito-Gutiérrez E (2025a) An ancient apical patterning system sets the position of the forebrain in chordates. *Sci. Adv* **11**:eadq4731 https://doi.org/10.1126/sciadv.adq4731 | PubMed

Gattoni G, Lin C.-Y, York JR, Shew C, Keitley D, LaBonne C, Yu J.-K, Gillis JA, Benito-Gutiérrez E (2025b) Evolutionary dynamics of FoxQ2 transcription factors across metazoans reveals three ancient paralogs. *Commun*. *Biol* **9**:98 https://doi.org/10.1038/s42003-025-09368-y | PubMed

Gehring WJ, Ikeo K (1999) Pax 6: mastering eye morphogenesis and eye evolution. *Trends Genet* **15**:371-377 https://doi.org/10.1016/s0168-9525(99)01776-x | PubMed

Hartenstein V, Spindler S, Pereanu W, Fung S (2008) The development of the Drosophila larval brain. *Adv. Exp. Med. Biol* **628**:1-31 https://doi.org/10.1007/978-0-387-78261-4_1 | PubMed

Hartenstein V, Cruz L, Lovick JK, Guo M (2017) Developmental analysis of the dopamine-containing neurons of the *Drosophila* brain. *J. Comp. Neurol* **525**:363-379 https://doi.org/10.1002/cne.24069 | PubMed

He B (2019) The role of Tc-foxQ2 in the central brain development in Tribolium castaneum. Göttingen University.

He B, Buescher M, Farnworth MS, Strobl F, Stelzer EH, Koniszewski ND, Muehlen D, Bucher G (2019) An ancestral apical brain region contributes to the central complex under the control of foxQ2 in the beetle Tribolium. *eLife* **8**:e49065 https://doi.org/10.7554/eLife.49065 | PubMed

Heisenberg M (2003) Mushroom body memoir: from maps to models. *Nat. Rev. Neurosci* **4**:266-275 https://doi.org/10.1038/nrn1074 | PubMed

Hirth F, Kammermeier L, Frei E, Walldorf U, Noll M, Reichert H (2003) An urbilaterian origin of the tripartite brain: developmental genetic insights from Drosophila. *Development* **130**:2365-73 https://doi.org/10.1242/dev.00438 | PubMed

Hunnekuhl VS, Siemanowski J, Farnworth MS, He B, Bucher G (2020) Immunohistochemistry and Fluorescent Whole Mount RNA In Situ Hybridization in Larval and Adult Brains of Tribolium. *Methods Mol Biol* **2047**:233-251 https://doi.org/10.1007/978-1-4939-9732-9_13 | PubMed

Kandimalla P, Omoto JJ, Hong EJ, Hartenstein V (2023) Lineages to circuits: the developmental and evolutionary architecture of information channels into the central complex. *J. Comp. Physiol. A* **209**:679-720 https://doi.org/10.1007/s00359-023-01616-y | PubMed

Karapidaki I, Handberg-Thorsager M, Momose T, Yasuo H, Genikhovich G, Assaf S, Deleau C, Pang Y, Pavlich C, Lohmann B, *et al.* (2025) A toolkit for testing membrane-localising tags across species. *bioRxiv* https://doi.org/10.1101/2024.11.12.623055

Kitzmann P, Weißkopf M, Schacht MI, Bucher G (2017) A key role for *foxQ2* in anterior head and central brain patterning in insects. *Development* **144**:2969-2981 https://doi.org/10.1242/dev.147637 | PubMed

Klingler M, Bucher G (2022) The red flour beetle T. castaneum: elaborate genetic toolkit and unbiased large scale RNAi screening to study insect biology and evolution. *EvoDevo* **13**:14 https://doi.org/10.1186/s13227-022-00201-9 | PubMed

Koniszewski NDB, Kollmann M, Bigham M, Farnworth M, He B, Büscher M, Hütteroth W, Binzer M, Schachtner J, Bucher G (2016) The insect central complex as model for heterochronic brain development—background, concepts, and tools. *Dev. Genes Evol* **226**:209-219 https://doi.org/10.1007/s00427-016-0542-7 | PubMed

Kunz T, Kraft KF, Technau GM, Urbach R (2012) Origin of *Drosophila* mushroom body neuroblasts and generation of divergent embryonic lineages. *Development* **139**:2510-2522 https://doi.org/10.1242/dev.077883 | PubMed

Leclère L, Bause M, Sinigaglia C, Steger J, Rentzsch F (2016) Development of the aboral domain in Nematostella requires β-catenin and the opposing activities of Six3/6 and Frizzled5/8. *Dev. Camb. Engl* **143**:1766-1777 https://doi.org/10.1242/dev.120931 | PubMed

Lee H, Frasch M (2004) Survey of forkhead domain encoding genes in the *Drosophila* genome: Classification and embryonic expression patterns. *Dev. Dyn* **229**:357-366 https://doi.org/10.1002/dvdy.10443 | PubMed

Li F, Lindsey JW, Marin EC, Otto N, Dreher M, Dempsey G, Stark I, Bates AS, Pleijzier MW, Schlegel P, *et al.* (2020) The connectome of the adult Drosophila mushroom body provides insights into function. *eLife* **9**:e62576 https://doi.org/10.7554/eLife.62576 | PubMed

Lillvis JL, Otsuna H, Ding X, Pisarev I, Kawase T, Colonell J, Rokicki K, Goina C, Gao R, Hu A, *et al.* (2022) Rapid reconstruction of neural circuits using tissue expansion and light sheet microscopy. *eLife* **11**:e81248 https://doi.org/10.7554/eLife.81248 | PubMed

Livet J, Weissman TA, Kang H, Draft RW, Lu J, Bennis RA, Sanes JR, Lichtman JW (2007) Transgenic strategies for combinatorial expression of fluorescent proteins in the nervous system. *Nature* **450**:56-62 https://doi.org/10.1038/nature06293 | PubMed

Mao Z, Davis RL (2009) Eight different types of dopaminergic neurons innervate the Drosophila mushroom body neuropil: anatomical and physiological heterogeneity. *Front. Neural Circuits* **3** https://doi.org/10.3389/neuro.04.005.2009 | PubMed

Marlow H, Tosches MA, Tomer R, Steinmetz PR, Lauri A, Larsson T, Arendt D (2014) Larval body patterning and apical organs are conserved in animal evolution. *BMC Biol* **12**:7 https://doi.org/10.1186/1741-7007-12-7 | PubMed

Miyares RL, Lee T (2019) Temporal control of Drosophila central nervous system development. *Curr. Opin. Neurobiol* **56**:24-32 https://doi.org/10.1016/j.conb.2018.10.016 | PubMed

Namiki S, Dickinson MH, Wong AM, Korff W, Card GM (2018) The functional organization of descending sensory-motor pathways in Drosophila. *eLife* **7**:e34272 https://doi.org/10.7554/eLife.34272 | PubMed

Ogawa Y, Shiraki T, Fukada Y, Kojima D (2021) Foxq2 determines blue cone identity in zebrafish. *Sci. Adv* **7**:eabi9784 https://doi.org/10.1126/sciadv.abi9784 | PubMed

Özel MN, Gibbs CS, Holguera I, Soliman M, Bonneau R, Desplan C (2022) Coordinated control of neuronal differentiation and wiring by sustained transcription factors. *Science* **378**:eadd1884 https://doi.org/10.1126/science.add1884 | PubMed

Pfeiffer K, Homberg U (2014) Organization and Functional Roles of the Central Complex in the Insect Brain. *Annu. Rev. Entomol* **59**:165-184 https://doi.org/10.1146/annurev-ento-011613-162031 | PubMed

Posnien N, Schinko JB, Kittelmann S, Bucher G (2010) Genetics, development and composition of the insect head – A beetle's view. *Arthropod Struct. Dev* **39**:399-410 https://doi.org/10.1016/j.asd.2010.08.002 | PubMed

Posnien N, Koniszewski N, Bucher G (2011) Insect Tc-six4 marks a unit with similarity to vertebrate placodes. *Dev. Biol* **350**:208-216 https://doi.org/10.1016/j.ydbio.2010.10.024 | PubMed

Posnien N, Hunnekuhl VS, Bucher G (2023) Gene expression mapping of the neuroectoderm across phyla – conservation and divergence of early brain anlagen between insects and vertebrates. *eLife* **12**:e92242 https://doi.org/10.7554/eLife.92242 | PubMed

Rethemeier S, Fritzsche S, Mühlen D, Bucher G, Hunnekuhl VS (2025) Differences in size and number of embryonic type II neuroblast lineages correlate with divergent timing of central complex development between beetle and fly. *eLife* **13**:RP99717 https://doi.org/10.7554/elife.99717 | PubMed

Sarrazin AF, Peel AD, Averof M (2012) A Segmentation Clock with Two-Segment Periodicity in Insects. *Science* https://doi.org/10.1126/science.1218256 | PubMed

Scaplen KM, Talay M, Nunez KM, Salamon S, Waterman AG, Gang S, Song SL, Barnea G, Kaun KR (2020) Circuits that encode and guide alcohol-associated preference. *eLife* **9**:e48730 https://doi.org/10.7554/eLife.48730 | PubMed

Schacht MI, Schomburg C, Bucher G (2020) six3 acts upstream of foxQ2 in labrum and neural development in the spider Parasteatoda tepidariorum. *Dev. Genes Evol* **230**:95-104 https://doi.org/10.1007/s00427-020-00654-9 | PubMed

Scheffer LK, Xu CS, Januszewski M, Lu Z, Takemura S.-Y, Hayworth KJ, Huang GB, Shinomiya K, Maitlin-Shepard J, Berg S, *et al.* (2020) A connectome and analysis of the adult Drosophila central brain. *eLife* **9**:e57443 https://doi.org/10.7554/eLife.57443 | PubMed

Schindelin J, Arganda-Carreras I, Frise E, Kaynig V, Longair M, Pietzsch T, Preibisch S, Rueden C, Saalfeld S, Schmid B, *et al.* (2012) Fiji: an open-source platform for biological-image analysis. *Nat. Methods* **9**:676-682 https://doi.org/10.1038/nmeth.2019 | PubMed

Schlegel P, Yin Y, Bates AS, Dorkenwald S, Eichler K, Brooks P, Han DS, Gkantia M, Dos Santos M, Munnelly EJ, *et al.* (2024) Whole-brain annotation and multi-connectome cell typing of Drosophila. *Nature* **634**:139-152 https://doi.org/10.1038/s41586-024-07686-5 | PubMed

Scholtz G, Edgecombe GD (2006) The evolution of arthropod heads: reconciling morphological, developmental and palaeontological evidence. *Dev Genes Evol* **216**:395-415 https://doi.org/10.1007/s00427-006-0085-4 | PubMed

Schomburg C (2010) Etablierung des Brainbow-Systems in Triboliuim.

Simeone A, Gulisano M, Acampora D, Stornaiuolo A, Rambaldi M, Boncinelli E (1992) Two vertebrate homeobox genes related to the Drosophila empty spiracles gene are expressed in the embryonic cerebral cortex. *Embo J* **11**:2541-50 https://doi.org/10.1002/j.1460-2075.1992.tb05319.x | PubMed

Sinigaglia C, Busengdal H, Leclère L, Technau U, Rentzsch F (2013) The Bilaterian Head Patterning Gene six3/6 Controls Aboral Domain Development in a Cnidarian. *PLoS Biol* **11**:e1001488 https://doi.org/10.1371/journal.pbio.1001488 | PubMed

Sinigaglia C, Almazán A, Lebel M, Sémon M, Gillet B, Hughes S, Edsinger E, Averof M, Paris M (2022) Distinct gene expression dynamics in developing and regenerating crustacean limbs. *Proc. Natl. Acad. Sci. U. S. A* **119**:e2119297119 https://doi.org/10.1073/pnas.2119297119 | PubMed

Skeath JB, Thor S (2003) Genetic control of Drosophila nerve cord development. *Curr. Opin. Neurobiol* **13**:8-15 https://doi.org/10.1016/s0959-4388(03)00007-2 | PubMed

Technau GM, Berger C, Urbach R (2006) Generation of cell diversity and segmental pattern in the embryonic central nervous system of Drosophila. *Dev Dyn* **235**:861-9 https://doi.org/10.1002/dvdy.20566 | PubMed

Tomer R, Denes AS, Tessmar-Raible K, Arendt D (2010) Profiling by image registration reveals common origin of annelid mushroom bodies and vertebrate pallium. *Cell* **142**:800-9 https://doi.org/10.1016/j.cell.2010.07.043 | PubMed

Truman JW, Riddiford LM (2023) Drosophila postembryonic nervous system development: a model for the endocrine control of development. *Genetics* **223**:iyac184 https://doi.org/10.1093/genetics/iyac184 | PubMed

Truman JW, Moats W, Altman J, Marin EC, Williams DW (2010) Role of Notch signaling in establishing the hemilineages of secondary neurons in *Drosophila melanogaster*. *Development* **137**:53-61 https://doi.org/10.1242/dev.041749 | PubMed

Urbach R, Technau GM (2003a) Early steps in building the insect brain: neuroblast formation and segmental patterning in the developing brain of different insect species. *Arthropod Struct. Dev* **32**:103-123 https://doi.org/10.1016/s1467-8039(03)00042-2 | PubMed

Urbach R, Technau GM (2003b) Segment polarity and DV patterning gene expression reveals segmental organization of the *Drosophila* brain. *Development* **130**:3607-3620 https://doi.org/10.1242/dev.00532 | PubMed

Urbach R, Technau GM (2004) Neuroblast formation and patterning during early brain development in *Drosophila*. *BioEssays* **26**:739-751 https://doi.org/10.1002/bies.20062 | PubMed

Urbach R, Schnabel R, Technau GM (2003) The pattern of neuroblast formation, mitotic domains and proneural gene expression during early brain development in *Drosophila*. *Development* **130**:3589-3606 https://doi.org/10.1242/dev.00528 | PubMed

Walsh KT, Doe CQ (2017) Drosophila embryonic type II neuroblasts: origin, temporal patterning, and contribution to the adult central complex. *Dev. Camb. Engl* **144**:4552-4562 https://doi.org/10.1242/dev.157826 | PubMed

Willig KI, Kellner RR, Medda R, Hein B, Jakobs S, Hell SW (2006) Nanoscale resolution in GFP-based microscopy. *Nat. Methods* **3**:721-723 https://doi.org/10.1038/nmeth922 | PubMed

Yaguchi S, Yaguchi J, Angerer RC, Angerer LM (2008) A Wnt-FoxQ2-Nodal Pathway Links Primary and Secondary Axis Specification in Sea Urchin Embryos. *Dev. Cell* **14**:97-107 https://doi.org/10.1016/j.devcel.2007.10.012 | PubMed

Yaguchi J, Takeda N, Inaba K, Yaguchi S (2016) Cooperative Wnt-Nodal Signals Regulate the Patterning of Anterior Neuroectoderm. *PLoS Genet* **12**:e1006001 https://doi.org/10.1371/journal.pgen.1006001 | PubMed

Peer reviews

Reviewer #1 (Public review):

Summary:

Pang et al. investigated the expression pattern of the transcription factor foxQ2II in an adult beetle brain. They find nine distinct clusters, with many neurons expressing Glut/ChaT and dopamine. Some of the dopamine neurons resemble cell types described in Drosophila. Several neurons seem to project to prominent higher brain regions such as the MB and CX, and might even connect to both.

Strengths:

The authors use state-of-the-art labeling techniques for the analysis of individual cell types, such as beetle brainbow, to investigate the until now unknown expression of the transcription factor in the adult beetle brain.

Rigorous cell reconstruction and image analysis revealed a better understanding of the anatomy of the labeled cells.

Weaknesses:

The brainbow labeling seems to include all cells labeled by the enhancer trap line, as well as the ones not expressing foxQ2II. Thus, it is unclear how useful this data is to compare individual cells to other insects.

The functional relevance of this transcription factor in the adult brain cell is still unknown. It is therefore unclear if the described neurons have any specific function and if they require this transcription factor for normal function.

Overall, the neural reconstructions are missing single-neuron details; it is difficult to compare the shown cell types to specific cell types in Drosophila based on the presented data, and this finding remains speculative.

https://doi.org/10.7554/eLife.111703.1.sa2

Reviewer #2 (Public review):

Summary:

The authors provide the first thorough profiling of neurons in Tribolium characterized by the expression of the transcription factor foxQ2, which will be useful for developmental neurobiology. They use state-of-the-art methods convincingly to not only identify the neurons, but also to further characterize them anatomically and neurochemically.

Strengths:

Thorough and meticulous application of state-of-the-art anatomical methods in a non-standard laboratory organism.

Weaknesses:

No weaknesses were identified by this reviewer.

Comments:

I don't really have any major suggestions at all. Loved the work.

There is only one tiny nitpicking aspect:

P21: "Biogenic amines are involved in learning and memory and setting arousal threshholds (Davis, 2023), which are functions performed by the mushroom bodies and related to the function of the central complex in goal directed navigation, respectively."

MBs mainly process olfactory memory. At least in Drosophila, most other kinds of memories are being supported elsewhere.

https://pubmed.ncbi.nlm.nih.gov/10454381/

such as, e.g., visual pattern learning in the CX

https://pubmed.ncbi.nlm.nih.gov/16452971/

or motor learning in motor neurons

https://pubmed.ncbi.nlm.nih.gov/38779314/

or ventral ganglion, antennal lobes, and median bundle for place learning:

https://pubmed.ncbi.nlm.nih.gov/10706599/

If the authors focus on MBs, this sentence ought to reflect the fact that the function of the MBs is much narrower than the current sentence appears to suggest.

https://doi.org/10.7554/eLife.111703.1.sa1

Author response:

We thank the editors and reviewers for their thoughtful and constructive assessment of Toothy, and for recognizing it as a potentially valuable resource for standardizing dentate spike (DS) analysis across labs. We are especially glad that the reviewers found the manuscript clear and easy to follow, judged the detection and classification algorithms to be appropriate and well-validated, and appreciated the tool's graphical user interface (GUI) based, pip-installable design for lowering the barrier to entry for DS analysis.

We also understand the concerns raised. Most importantly, we will resolve the data-ingestion and classification errors that reviewers encountered and release an updated version of Toothy that we have verified end-to-end across input formats and datasets. Alongside this, we will provide downloadable demo dataset(s) spanning multiple file formats, probe types, and recording conditions, so that users can confirm a correct installation and see how these cases differ.

To make the pipeline more transparent, we will add a section describing what Toothy does between user steps, including the rationale for decisions users cannot change, such as detection from a single representative channel. We will also expand the documentation of parameter choices with supporting citations and alternatives, and surface this guidance within Toothy where feasible, consistent with our aim that the tool not function as a black box.

We will clarify Toothy's scope and current limitations. Recordings with irregular spatial sampling (e.g., tetrodes) are supported for detection but not for CSD-based DS-type classification, which requires a laminar probe spanning approximately the hippocampal fissure to the hilus; we will state this explicitly and evaluate adding an optional waveform-based classification mode (Santiago et al., 2024) to extend type classification to such recordings. We will also add data-quality checks (including sampling rate and inter-electrode spacing) that warn users when a recording may not support reliable results.

Finally, we will situate Toothy among existing open-source toolboxes, describing how it differs, extends beyond, and interoperates with them, and we will add a comparison of Toothy's outputs to previously published analyses while being explicit about the limits of such comparisons. We will of course also address the remaining technical clarifications and figure edits raised by the reviewers.

We are confident that addressing these points will make Toothy clearer and more useful to the hippocampal community.

https://doi.org/10.7554/eLife.111703.1.sa0